

GIBBS MEASURES OF POTTS MODEL ON CAYLEY TREES: A SURVEY AND APPLICATIONS

U.A. ROZIKOV

ABSTRACT. In this paper we give a systematic review of the theory of Gibbs measures of Potts model on Cayley trees (developed since 2013) and discuss many applications of the Potts model to real world situations: mainly biology, physics, and some examples of alloy behavior, cell sorting, financial engineering, flocking birds, flowing foams, image segmentation, medicine, sociology etc.

1. INTRODUCTION

The Potts model is defined by a Hamiltonian (energy) of configurations of spins which take one of q possible values on vertices of a lattice. The model is used to study the behavior of systems having multiple states (spins, colors, alleles, etc). Since the model has a rich mathematical formulation it has been studied extensively.

Usually the results of investigations of a system (in particular, the Potts model) are presented by a measure assigning a number to each (interesting) suitable properties of the system. The Gibbs measure is one of such important measures in many problems of probability theory and statistical mechanics. It is the measure associated with the Hamiltonian of a (biological, physical) system. Each Gibbs measure gives a state of the system.

The main problem for a given Hamiltonian on a countable lattice is to describe its all possible Gibbs measures. In case of uniqueness of the Gibbs measure (for all values of the parameters, in particular a parameter can be temperature), the system does not change its state. The existence of some values of parameters at which the uniqueness of Gibbs measure switches to non-uniqueness is interpreted as phase transition (the system will change its state).

The book [103] presents all known (since 2012) mathematical results on (extreme) Gibbs measures on Cayley trees. At that time, the Potts model on trees was not well studied, compared to the Ising model. Even results about translation-invariant (simple) Gibbs measures were not complete and periodic Gibbs measures were not studied.

First complete result about translation-invariant Gibbs measures of the Potts model on Cayley trees appeared in 2014, [50]. Periodic and weakly periodic measures were studied after 2015. These results mainly have applications to physics as thermodynamical systems.

In this review, I have collected all these recent results and have presented many applications in biology, medicine, sociology, physics etc.

2020 *Mathematics Subject Classification.* 82B20 (82B26).

Key words and phrases. Cayley tree, configuration, Potts model, temperature, Gibbs measure.

2. PRELIMINARIES

The Cayley tree Γ^k : The Cayley tree Γ^k of order $k \geq 1$ is an infinite tree, i.e., a graph without cycles, such that exactly $k + 1$ edges originate from each vertex. Let $\Gamma^k = (V, L, i)$, where V is the set of vertices Γ^k , L the set of edges and i is the incidence function setting each edge $l \in L$ into correspondence with its endpoints $x, y \in V$. If $i(l) = \{x, y\}$, then the vertices x and y are called the *nearest neighbors*, denoted by $l = \langle x, y \rangle$.

Fix a vertex $x^0 \in V$, interpreted as the *root* of the tree. We say that $y \in V$ is a *direct successor* of $x \in V$ if x is the penultimate vertex on the unique path leading from the root x^0 to the vertex y ; that is, $d(x^0, y) = d(x^0, x) + 1$ and $d(x, y) = 1$. The set of all direct successors of $x \in V$ is denoted $S(x)$.

For a fixed $x^0 \in V$ we set $W_n = \{x \in V \mid d(x, x^0) = n\}$,

$$V_n = \{x \in V \mid d(x, x^0) \leq n\}, \quad L_n = \{l = \langle x, y \rangle \in L \mid x, y \in V_n\}. \quad (2.1)$$

For $x \in W_n$ the set $S(x)$ then has the form

$$S(x) = \{y \in W_{n+1} : \langle x, y \rangle\}. \quad (2.2)$$

For any $x \in V$ denote

$$W_m(x) = \{y \in V : d(x, y) = m\}, \quad m \geq 1.$$

Note that the sequence of balls (V_n) ($n \in \mathbb{N}_0$) is *cofinal* (see [36, Section 1.2, page 17]), that is, any finite subset $A \subset V$ is contained in some V_n .

Group representation of the tree.

Let G_k be a free product of $k + 1$ cyclic groups of the second order with generators a_1, a_2, \dots, a_{k+1} , respectively, i.e. $a_i^2 = e$, where e is the unit element.

It is known that there exists a one-to-one correspondence between the set of vertices V of the Cayley tree Γ^k and the group G_k (see Chapter 1 of [103] for properties of the group G_k).

Consideration of the Cayley trees has many motivations (see e.g. [12], [21], [22], [35], [69], [109], [112] and references therein).

Configuration space: Take a finite set $\Phi = \{1, 2, \dots, q\}$, $q \geq 2$. This is the set of spin values. For $A \subseteq V$ a spin *configuration* σ_A on A is defined as a function

$$x \in A \rightarrow \sigma_A(x) \in \Phi.$$

The set of all configurations coincides with $\Omega_A = \Phi^A$. The cardinality of Ω_A is $|\Omega_A| = |\Phi|^{|A|} = q^{|A|}$.

We denote $\Omega = \Omega_V$ and $\sigma = \sigma_V$. Since V is a countable set, Ω is an uncountable set.

Let G^* be a subgroup of the group G_k . A configuration $\sigma \in \Omega$ is called G^* -periodic if $\sigma(yx) = \sigma(x)$ for any $x \in G_k$ and $y \in G^*$.

A configuration that is invariant with respect to all shifts is called *translation-invariant*.

The q -state Potts model: Consider the Potts model, where the spin at each vertex $x \in V$ can take values in the set $\Phi := \{1, \dots, q\}$.

The Potts model with a *nearest-neighbour interaction kernel* $\{J_{xy}\}_{x,y \in V}$ (i.e., such that $J_{xy} = J_{yx}$ and $J_{xy} = 0$ if $d(x, y) \neq 1$) is defined by the formal Hamiltonian

$$H(\sigma) = - \sum_{\langle x, y \rangle \in L} J_{xy} \delta_{\sigma(x), \sigma(y)} - \sum_{x \in V} \xi_{\sigma(x)}(x), \quad \sigma \in \Phi^V, \quad (2.3)$$

where δ_{ij} is the Kronecker delta symbol, i.e.,

$$\delta_{ij} = \begin{cases} 1, & \text{if } i = j \\ 0, & \text{if } i \neq j \end{cases}$$

and $\xi(x) = (\xi_1(x), \dots, \xi_q(x)) \in \mathbb{R}^q$ is the external (possibly random) field.

For $q = 2$, the Potts model is equivalent to the Ising model (see Chapter 2 of [103]).

Gibbs measure for the Potts model: For each finite subset $\Lambda \subset V$ ($\Lambda \neq \emptyset$) and any fixed sub-configuration $\eta \in \Phi^{\Lambda^c}$ (called the *configurational boundary condition*), the *Gibbs measure* γ_Λ^η is a probability measure in Φ^Λ defined by the formula

$$\gamma_\Lambda^\eta(\varsigma) = \frac{1}{Z_\Lambda^\eta(\beta)} \exp \left\{ -\beta H_\Lambda(\varsigma) + \beta \sum_{x \in \Lambda} \sum_{y \in \Lambda^c} J_{xy} \delta_{\varsigma(x), \eta(y)} \right\}, \quad \varsigma \in \Phi^\Lambda, \quad (2.4)$$

where H_Λ is the restriction of the Hamiltonian (2.3) to configurations in Λ ,

$$H_\Lambda(\varsigma) = - \sum_{\langle x, y \rangle \in L_\Lambda} J_{xy} \delta_{\varsigma(x), \varsigma(y)} - \sum_{x \in \Lambda} \xi_{\varsigma(x)}(x), \quad \varsigma \in \Phi^\Lambda, \quad (2.5)$$

and $Z_\Lambda^\eta(\beta)$ is the partition function (or normalizing constant)

$$Z_\Lambda^\eta(\beta) = \sum_{\varsigma \in \Phi^\Lambda} \exp \left\{ -\beta H_\Lambda(\varsigma) + \beta \sum_{x \in \Lambda} \sum_{y \in \Lambda^c} J_{xy} \delta_{\varsigma(x), \eta(y)} \right\}.$$

Now a measure $\mu = \mu_{\beta, \xi}$ on Φ^V is called a *Gibbs measure* if, for any non-empty finite set $\Lambda \subset V$ and any $\eta \in \Phi^{\Lambda^c}$,

$$\mu(\sigma_\Lambda = \varsigma \mid \sigma_{\Lambda^c} = \eta) \equiv \gamma_\Lambda^\eta(\varsigma), \quad \varsigma \in \Phi^\Lambda. \quad (2.6)$$

The main problem: is to study the structure of the set $\mathcal{G}(H)$ of all Gibbs measures corresponding to a given Hamiltonian H .

The existence of Gibbs measures for a wide class of Hamiltonians was established in the ground-breaking work of Dobrushin (see, e.g., [36], [27], [120]). However, a complete analysis of the set of Gibbs measures for a given Hamiltonian is often a difficult problem.

A measure $\mu \in \mathcal{G}(H)$ is called *extreme* (also called pure state) if it cannot be expressed as $\mu = \lambda \mu_1 + (1 - \lambda) \mu_2$ for some $\mu_1, \mu_2 \in \mathcal{G}(H)$ with $\mu_1 \neq \mu_2$.

The set of all extreme measures in $\mathcal{G}(H)$ denoted by $\text{ex}\mathcal{G}(H)$ is a *Choquet simplex*, in the sense that any $\mu \in \mathcal{G}(H)$ can be represented as $\mu = \int_{\text{ex}\mathcal{G}(H)} \nu \rho(d\nu)$, with some probability measure ρ on $\text{ex}\mathcal{G}(H)$.

Thus the analysis of $\mathcal{G}(H)$ is reduced to description of its extremal elements. Extremal Gibbs measures are very important to understanding all possible local behaviors of the (biological and physical) system.

In this paper we give some extreme points of the set of Gibbs measures for the Potts model.

A method to describe Gibbs measure on trees: Follow [10] and [51] to explain the method of Markov random field theory and its recurrent equations.

For a vector field $V \ni x \mapsto \mathbf{h}(x) = (h_1(x), \dots, h_q(x)) \in \mathbb{R}^q$ and each $n \in \mathbb{N}_0 = \{0, 1, \dots\}$, define a probability measure in Φ^{V_n} by the formula

$$\mu_n^h(\sigma_n) = \frac{1}{Z_n} \exp \left\{ -\beta H_n(\sigma_n) + \beta \sum_{x \in W_n} h_{\sigma_n(x)}(x) \right\}, \quad \sigma_n \in \Phi^{V_n}, \quad (2.7)$$

where $Z_n = Z_n(\beta, \mathbf{h})$ is the normalizing factor and $H_n := H_{V_n}$, that is (see (2.5)),

$$H_n(\sigma_n) = - \sum_{\langle x, y \rangle \in L_n} J_{xy} \delta_{\sigma_n(x), \sigma_n(y)} - \sum_{x \in V_n} \xi_{\sigma_n(x)}(x), \quad \sigma_n \in \Phi^{V_n}. \quad (2.8)$$

The vector field $\{\mathbf{h}(x)\}_{x \in V}$ in (2.7) is called *generalized boundary conditions (GBC)*.

One says that the probability distributions (2.7) are *compatible* (and the intrinsic GBC $\{\mathbf{h}(x)\}$ are *permissible*) if for each $n \in \mathbb{N}_0$ the following identity holds,

$$\sum_{\omega \in \Phi^{W_{n+1}}} \mu_{n+1}^h(\sigma_n \vee \omega) \equiv \mu_n^h(\sigma), \quad \sigma_n \in \Phi^{V_n}, \quad (2.9)$$

where the symbol \vee stands for concatenation of sub-configurations.

By Kolmogorov's extension theorem (see, e.g., [27], [119, Chapter II, §3, Theorem 4, page 167] and more suitable for our setting is [27, Theorem 6.2]), the compatibility condition (2.9) ensures that there exists a unique measure $\mu^h = \mu_{\beta, \xi}^h$ on Φ^V such that, for all $n \in \mathbb{N}_0$,

$$\mu^h(\sigma_{V_n} = \sigma_n) \equiv \mu_n^h(\sigma_n), \quad \sigma_n \in \Phi^{V_n}, \quad (2.10)$$

or more explicitly (substituting (2.7)),

$$\mu^h(\sigma_{V_n} = \sigma_n) = \frac{1}{Z_n} \exp \left\{ -\beta H_n(\sigma_n) + \beta \sum_{x \in W_n} h_{\sigma_n(x)}(x) \right\}, \quad \sigma_n \in \Phi^{V_n}. \quad (2.11)$$

Definition 2.1. Measure μ^h satisfying (2.10) is called a *splitting Gibbs measure (SGM)*.

Remark 2.1. Note that adding a constant $c = c(x)$ to all coordinates $h_i(x)$ of the vector $\mathbf{h}(x)$ does not change the probability measure (2.7) due to the normalization Z_n . The same is true for the external field $\xi(x)$ in the Hamiltonian (2.8). Therefore, without loss of generality consider *reduced GBC* $\check{\mathbf{h}}(x)$, for example defined as

$$\check{h}_i(x) = h_i(x) - h_q(x), \quad i = 1, \dots, q-1.$$

The same remark also applies to the external field ξ and its reduced version $\check{\xi}(x)$, defined by

$$\check{\xi}_i(x) := \xi_i(x) - \xi_q(x), \quad i = 1, \dots, q-1.$$

Such a reduction can equally be done by subtracting any other coordinate,

$${}_{\ell} \check{h}_i(x) := h_i(x) - h_{\ell}(x), \quad {}_{\ell} \check{\xi}_i(x) := \xi_i(x) - \xi_{\ell}(x) \quad (i \neq \ell).$$

Therefore, when working with vectors and vector-valued functions and fields it will often be convenient to pass from a generic vector $\mathbf{u} = (u_1, \dots, u_q)$ to a "reduced vector" $\check{\mathbf{u}} = (\check{u}_1, \dots, \check{u}_{q-1}) \in \mathbb{R}^{q-1}$ by setting $\check{u}_i := u_i - u_q$ ($i = 1, \dots, q-1$).

The following statement describes a criterion for the GBC $\{\mathbf{h}(x)\}_{x \in V}$ to guarantee compatibility of the measures $\{\mu_n^h\}_{n \in \mathbb{N}_0}$.

Theorem 2.1. (see [10]) *The probability distributions $\{\mu_n^h\}_{n \in \mathbb{N}_0}$ defined in (2.7) are compatible if and only if the following vector identity holds*

$$\beta \check{\mathbf{h}}(x) = \sum_{y \in S(x)} \mathbf{F}(\beta \check{\mathbf{h}}(y) + \beta \check{\boldsymbol{\xi}}(y); e^{\beta J_{xy}}), \quad x \in V, \quad (2.12)$$

where $\check{\mathbf{h}}(x) = (\check{h}_1(x), \dots, \check{h}_{q-1}(x))$, $\check{\boldsymbol{\xi}}(x) = (\check{\xi}_1(x), \dots, \check{\xi}_{q-1}(x))$,

$$\check{h}_i(x) := h_i(x) - h_q(x), \quad \check{\xi}_i(x) := \xi_i(x) - \xi_q(x), \quad i = 1, \dots, q-1, \quad (2.13)$$

and the map $\mathbf{F}(\mathbf{u}; \theta) = (F_1(\mathbf{u}; \theta), \dots, F_{q-1}(\mathbf{u}; \theta))$ is defined for $\mathbf{u} = (u_1, \dots, u_{q-1}) \in \mathbb{R}^{q-1}$ and $\theta > 0$ by the formulas

$$F_i(\mathbf{u}; \theta) := \ln \frac{(\theta - 1)e^{u_i} + 1 + \sum_{j=1}^{q-1} e^{u_j}}{\theta + \sum_{j=1}^{q-1} e^{u_j}}, \quad i = 1, \dots, q-1. \quad (2.14)$$

Now, using [36, Theorem (12.6)] and according to the link between GBC $\{\mathbf{h}(x)\}_{x \in V}$ and boundary laws (see [10, Remark 1.4]) we make the following **crucial observations**:

- *any extreme measure $\mu \in \text{ex}\mathcal{G}(H)$ is SGM*; therefore, the question of uniqueness of the Gibbs measure is reduced to that in the SGM class. Moreover, for each given temperature, the description of the set $\mathcal{G}(H)$ is equivalent to the full description of the set of all extreme SGMs. Therefore, in this paper we only interested to SGM on the Cayley trees.
- *Any SGM corresponds to a solution of (2.12) given in Theorem 2.1.* Thus our main problem is reduced to solving the functional equation (2.12) and to check when a SGM corresponding to a solution is extreme.

To check the extremality of a Gibbs measure one can apply arguments used for the reconstruction on trees [25], [44], [63], [68], [69].

It is also known that a sufficient condition for non-extremality (which is equivalent to solvability of the associated reconstruction) of a Gibbs measure is the Kesten-Stigum condition given in [44].

3. TRANSLATION-INVARIANT SGMs.

In this section we consider the classic version of the Potts model:

$$H(\sigma) = -J \sum_{\langle x, y \rangle \in L} \delta_{\sigma(x)\sigma(y)}, \quad (3.1)$$

where $J \in \mathbb{R}$, $\sigma(x) \in \Phi = \{1, \dots, q\}$ and $\langle x, y \rangle$ stands for nearest neighbor vertices.

Let S_q be the group of permutations on Φ .

Take $\sigma \in \Phi^V$ and define an action of $\pi = (\pi_1, \dots, \pi_q) \in S_q$ on σ (denoted by $\pi\sigma$) as

$$(\pi\sigma)(x) = \pi_{\sigma(x)}, \quad \text{for all } x \in V.$$

Then it is easy to see that for any $\sigma \in \Phi^V$ and any $\pi \in S_q$ we have $H(\pi\sigma) = H(\sigma)$.

By Theorem 2.1 to each splitting Gibbs measure (SGM) of the Hamiltonian (3.1) there is a vector-valued function h_x , such that for any $x \in V \setminus \{x^0\}$ the following equation holds:

$$h_x = \sum_{y \in S(x)} F(h_y, \theta), \quad (3.2)$$

where $F : h = (h_1, \dots, h_{q-1}) \in \mathbb{R}^{q-1} \rightarrow F(h, \theta) = (F_1, \dots, F_{q-1}) \in \mathbb{R}^{q-1}$ is defined as

$$F_i = \ln \left(\frac{(\theta - 1)e^{h_i} + \sum_{j=1}^{q-1} e^{h_j} + 1}{\theta + \sum_{j=1}^{q-1} e^{h_j}} \right),$$

$\theta = \exp(J\beta)$, $S(x)$ is the set of direct successors of x and $h_x = (h_{1,x}, \dots, h_{q-1,x})$ with

$$h_{i,x} = \tilde{h}_{i,x} - \tilde{h}_{q,x}, \quad i = 1, \dots, q-1. \quad (3.3)$$

Moreover, for any $h = \{h_x, x \in V\}$ satisfying (3.2) there exists a unique SGM μ for the Potts model.

In this section, we review main results of [50]. Consider SGMs which are translation-invariant, i.e., assume $h_x = h = (h_1, \dots, h_{q-1}) \in \mathbb{R}^{q-1}$ for all $x \in V$. Then from equation (3.2) we get $h = kF(h, \theta)$, i.e.,

$$h_i = k \ln \left(\frac{(\theta - 1)e^{h_i} + \sum_{j=1}^{q-1} e^{h_j} + 1}{\theta + \sum_{j=1}^{q-1} e^{h_j}} \right), \quad i = 1, \dots, q-1. \quad (3.4)$$

Denoting $z_i = \exp(h_i)$, $i = 1, \dots, q-1$, from (3.4) we get

$$z_i = \left(\frac{(\theta - 1)z_i + \sum_{j=1}^{q-1} z_j + 1}{\theta + \sum_{j=1}^{q-1} z_j} \right)^k, \quad i = 1, \dots, q-1. \quad (3.5)$$

Remark 3.1. The permutation symmetry of Hamiltonian (3.1) mentioned above consequences such symmetry to solutions of (5.2): if $z = (z_1, \dots, z_{q-1})$ is a solution to (5.2) then by any permutation of its coordinates we get a solution of (5.2) too.

It is known that if $J < 0$ (i.e. $\theta < 1$) then for any $k \geq 1$, $q \geq 2$ the anti-ferromagnetic Potts model has a unique TISGM (i.e., [103, p.109], [96]) i.e. the following theorem holds.

Theorem 3.1. *For the q -state anti-ferromagnetic ($J < 0$) Potts model on the Cayley tree of order $k \geq 2$ there is unique TISGM.*

The following theorem characterizes all solutions of (5.2).

Theorem 3.2. *For any solution $z = (z_1, \dots, z_{q-1})$ of the system of equations (5.2) there exists $M \subset \{1, \dots, q-1\}$ and $z^* > 0$ such that*

$$z_i = \begin{cases} 1, & \text{if } i \notin M \\ z^*, & \text{if } i \in M. \end{cases}$$

As a consequence of this theorem one can see that any TISGM of the Potts model corresponds to a solution of the following equation

$$z = f_m(z) \equiv \left(\frac{(\theta + m - 1)z + q - m}{mz + q - m - 1 + \theta} \right)^k, \quad (3.6)$$

for some $m = 1, \dots, q-1$.

Put

$$T_{cr} = \frac{J}{\ln \left(1 + \frac{q}{k-1} \right)}.$$

In [50] by analysis of solutions of the equation (3.6) the following theorem is proved.

Theorem 3.3. *For the q -state ferromagnetic ($J > 0$) Potts model on the Cayley tree of order $k \geq 2$ there are critical temperatures $T_{c,m} \equiv T_{c,m}(k, q)$, $m = 1, \dots, [q/2]$ such that the following statements hold*

1.

$$T_{c,1} > T_{c,2} > \dots > T_{c,[\frac{q}{2}]-1} > T_{c,[\frac{q}{2}]} \geq T_{cr};$$

2. *If $T > T_{c,1}$ then there exists a unique TISGM;*

3. *If $T_{c,m+1} < T < T_{c,m}$ for some $m = 1, \dots, [q/2] - 1$ then there are $1 + 2 \sum_{s=1}^m \binom{q}{s}$ TISGMs.*

4. *If $T_{cr} \neq T < T_{c,[\frac{q}{2}]}$ then there are $2^q - 1$ TISGMs.*

5. *If $T = T_{cr}$ then the number of TISGMs is as follows*

$$\begin{cases} 2^{q-1}, & \text{if } q - \text{odd} \\ 2^{q-1} - \binom{q-1}{q/2}, & \text{if } q - \text{even.} \end{cases};$$

6. *If $T = T_{c,m}$, $m = 1, \dots, [q/2]$, ($T_{c,[q/2]} \neq T_{cr}$) then there are $1 + \binom{q}{m} + 2 \sum_{s=1}^{m-1} \binom{q}{s}$ TISGMs.*

Remark 3.2. Let us make some useful remarks

1. The critical temperature $T_{cr} = \frac{J}{\ln(1 + \frac{q}{k-1})}$ is explicit for any $k \geq 2$ and any $q \geq 2$. For other critical values we know only existence and explicit formulas for $k = 2$:

$$T_{c,m} \equiv T_{c,m}(2, q) = \frac{J}{\ln(1 + 2\sqrt{m(q-m)})}, \quad m = 1, 2, \dots, [\frac{q}{2}]. \quad (3.7)$$

2. For the case $k = 2$, $q = 3$ we have two critical temperatures

$$T_{cr} = \frac{J}{\ln 4}, \quad T_{c,1} = \frac{J}{\ln(1 + 2\sqrt{2})},$$

and up to $2^3 - 1 = 7$ TISGMs, denoted by μ_i , $i = 0, \dots, 6$. Here, μ_0 is free measure, corresponding to solution 1. Each TISGM defines its own measure of the cylinder $\{\sigma \in \Omega : \sigma(x) = j\}$, $x \in V$, $j = 1, 2, 3$. Moreover, since these measures are translation invariant, the measure of this cylinder does not depend on $x \in V$:

$$\mu_i(\{\sigma \in \Omega : \sigma(x) = j\}) = p_{ij}.$$

Depending on the value of the solution z of (3.6) one can calculate p_{ij} . In case $z = 1$, $p_{0j} = 1/3$ (since $q = 3$). If μ_i corresponds to a solution $z > 1$ then for sufficiently low temperatures we have $p_{i1} > 2/3$, and for $z < 1$ we have $p_{i1} < 1/3$. Consequently, we can see typical configurations (of the seven TISGMs, i.e. phases) of the two-dimensional 3-state Potts model, for different values of temperature as shown in Fig. 1.

Theorem 3.4. *If $T \leq T_{c,1}$ then there are at least two extreme Gibbs measures for the q -state Potts model on the Cayley tree of order $k \geq 2$.*

Let \mathcal{G}_{ti} be the set of all TISGMs. The following gives relations between TISGMs.

Theorem 3.5. *Any measure $\mu \in \mathcal{G}_{ti}$ can not be non-trivial convex mixture of measures from $\mathcal{G}_{ti} \setminus \{\mu\}$.*

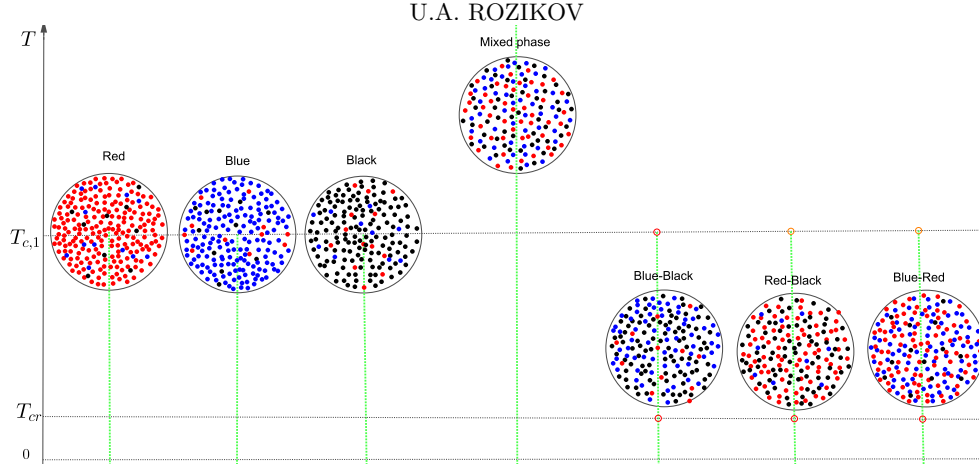


FIGURE 1. 3-state Potts model’s typical configurations depending on temperature. Here, states are: red=1, blue=2, black=3. All possible (seven) cases are shown: In the mixed phase all three colors are seen with equal probability (with respect to the unique TISGM, i.e. free Gibbs measure). The “Red” phase (having many reds and very few other colors) is the typical configuration for the TISGM corresponding to the solution $(z_2, 1, 1)$. Similarly, “Blue” and “Black” phases are the typical configurations for the TISGMs corresponding to the coordinate-permutations of $(z_2, 1, 1)$. The “Blue-Black” phase (having blue and black colors with equal probability, but very few red color) corresponds to $(z_1, 1, 1)$ and the remaining two phases correspond to its coordinate-permutations. Green vertical lines show the region of the temperature where the corresponding TISGM exists. At the red points (shown at critical temperatures) on the blue lines the TISGMs do not exist.

We now know that at sufficiently low temperatures the maximal number of TISGMs is $2^q - 1$. Moreover, it was shown that the number of TISGMs does not depend on the order $k \geq 2$ of the Cayley tree.

However it is not clear what kind of boundary conditions (configurations) are needed to get the TISGMs as corresponding limits with the boundary conditions.

In [29] we have answered this question.

Remark 3.3. 1. It is known (see ([36], [40])) that the set $\mathcal{G}(J)$ of all Gibbs measures (for a fixed parameter J of the Hamiltonian (3.1)) is a non-empty, compact convex set. A limiting Gibbs measure is a Gibbs measure for the same J . Conversely, every extremal point of $\mathcal{G}(J)$ is a limiting Gibbs measure with a suitable boundary condition for the same J .

2. It is known that any extreme Gibbs measure of a Hamiltonian with nearest-neighbor interactions is a *splitting* Gibbs measure. Consequently, any non-splitting Gibbs measure is not extreme. However, any splitting Gibbs measure (not necessary extreme) is a limiting Gibbs measure, because it corresponds to a (generalized)¹ boundary condition satisfying a compatibility (tree recursion) condition of Kolmogorov’s theorem.

¹Recall that added a boundary field at each site of the boundary is called a generalized boundary condition [28] or boundary law [36]

3. In [20] it was shown that for non-extremal Gibbs measures on \mathbb{Z}^d a Gibbs measure need not be a limiting Gibbs measure (see [20] and [27] for more details).

Consider the case $k = 2$. In this case it is known that (see [50]) for a given $m \leq \lfloor \frac{q}{2} \rfloor$, there are vector solutions

$$\underbrace{(h_i, h_i, \dots, h_i)}_m, \underbrace{(0, 0, \dots, 0)}_{q-m}$$

permuting coordinates of which one obtains $\binom{q}{m}$ TISGMs.

Thus without loss of generality we can only consider the measure $\mu_i(\theta, m)$ corresponding to vector

$$\mathbf{h}(m, i) = \underbrace{(h_i, h_i, \dots, h_i)}_m, \underbrace{(0, 0, \dots, 0)}_{q-m-1}.$$

Denote by $\mu_0 \equiv \mu_0(\theta)$ the TISGM corresponding to solution $h_i \equiv 0$ and by $\mu_i \equiv \mu_i(\theta, m)$ the TISGM corresponding to the solution $h_i(\theta, m)$, $i = 1, 2$, $m = 1, \dots, \lfloor \frac{q}{2} \rfloor$.

In [29] we have obtained all measures μ_i by changing boundary conditions (configurations). To give the main result of [29] we need the following result of [50]. Denote

$$\theta_m = 1 + 2\sqrt{m(q-m)}, \quad m = 1, \dots, q-1. \quad (3.8)$$

It is easy to see that

$$\theta_m = \theta_{q-m} \quad \text{and} \quad \theta_1 < \theta_2 < \dots < \theta_{\lfloor \frac{q}{2} \rfloor - 1} < \theta_{\lfloor \frac{q}{2} \rfloor} \leq q+1. \quad (3.9)$$

Denote

$$\begin{aligned} x_1(m) &= \frac{\theta - 1 - \sqrt{(\theta - 1)^2 - 4m(q-m)}}{2m}, \\ x_2(m) &= \frac{\theta - 1 + \sqrt{(\theta - 1)^2 - 4m(q-m)}}{2m}. \end{aligned} \quad (3.10)$$

Proposition 3.6. *Let $k = 2$, $J > 0$.*

1. *If $\theta < \theta_1$ then the system of equations (3.4) has a unique solution $h_0 = (0, 0, \dots, 0)$;*
2. *If $\theta_m < \theta < \theta_{m+1}$ for some $m = 1, \dots, \lfloor \frac{q}{2} \rfloor - 1$ then the system of equations (3.4) has solutions*

$$h_0 = (0, 0, \dots, 0), \quad h_{1i}(s), \quad h_{2i}(s), \quad i = 1, \dots, \binom{q-1}{s},$$

$$h'_{1i}(q-s), \quad h'_{2i}(q-s), \quad i = 1, \dots, \binom{q-1}{q-s}, \quad s = 1, 2, \dots, m,$$

where $h_{ji}(s)$, (resp. $h'_{ji}(q-s)$) $j = 1, 2$ is a vector with s (resp. $q-s$) coordinates equal to $2 \ln x_j(s)$ (resp. $2 \ln x_j(q-s)$) and the remaining $q-s-1$ (resp. $s-1$) coordinates equal to 0. The number of such solutions is equal to

$$1 + 2 \sum_{s=1}^m \binom{q}{s};$$

3. *If $\theta_{\lfloor \frac{q}{2} \rfloor} < \theta \neq q+1$ then there are $2^q - 1$ solutions to (3.4);*
4. *If $\theta = q+1$ then the number of solutions is as follows*

$$\begin{cases} 2^{q-1}, & \text{if } q \text{ is odd} \\ 2^{q-1} - \binom{q-1}{q/2}, & \text{if } q \text{ is even;} \end{cases}$$

5. If $\theta = \theta_m$, $m = 1, \dots, [\frac{q}{2}]$, ($\theta_{[\frac{q}{2}]} \neq q + 1$) then $h_{1i}(m) = h_{2i}(m)$. The number of solutions is equal to

$$1 + \binom{q}{m} + 2 \sum_{s=1}^{m-1} \binom{q}{s}.$$

Remark 3.4. We note that

- 1) By Proposition 3.6 for $k = 2$ and $J > 0$ we have the full description of solutions to the system of equations (3.4). Consequently, this gives the full description of TISGMs. Moreover, depending on parameter θ the maximal number of such measures can be $2^q - 1$.
- 2) Recall $\theta_c = \frac{k+q-1}{k-1}$, $k \geq 2$, $q \geq 2$. For $k = 2$ by (3.8) we have

$$\begin{cases} \theta_c > \theta_m, & \text{for all } m \in \{1, \dots, q-1\} \setminus \{q/2\} \\ \theta_c = \theta_m, & \text{for } m = q/2. \end{cases}$$

Let $\omega \in \Omega$ be a configuration such that

$$c^l(\omega) = \sum_{s \in S(t)} \delta_{l\omega(s)}$$

is independent of $t \in V \setminus \{x^0\}$.

For a given $m \in \{1, \dots, [\frac{q}{2}]\}$ and $J > 0$ introduce the following sets of configurations:

$$\begin{aligned} \mathbb{B}_m &= \{\omega \in \Omega : c^1(\omega) = \dots = c^m(\omega), \quad c^{m+1}(\omega) = \dots = c^{q-1}(\omega) = c^q(\omega)\}, \\ \mathbb{B}_{m,0}^+ &= \{\omega \in \mathbb{B}_m : c^1(\omega) > c^q(\omega)\}, \\ \mathbb{B}_{m,0}^0 &= \{\omega \in \mathbb{B}_m : c^1(\omega) = c^q(\omega)\}, \\ \mathbb{B}_{m,0}^- &= \{\omega \in \mathbb{B}_m : c^1(\omega) < c^q(\omega)\}, \\ \mathbb{B}_{m,1}^+ &= \{\omega \in \mathbb{B}_m : J(c^1(\omega) - c^q(\omega)) > h_1\}, \\ \mathbb{B}_{m,1}^0 &= \{\omega \in \mathbb{B}_m : J(c^1(\omega) - c^q(\omega)) = h_1\}, \\ \mathbb{B}_{m,1}^- &= \{\omega \in \mathbb{B}_m : J(c^1(\omega) - c^q(\omega)) < h_1\}. \end{aligned}$$

Denote by P^ω the limiting Gibbs measure corresponding to a boundary configuration ω . The main result of [29] is the following

Theorem 3.7. *The following assertions hold*

1) If $\theta = \theta_m$, for some $m = 1, \dots, [\frac{q}{2}]$ then

$$P^\omega = \begin{cases} \mu_1(\theta, m), & \text{if } \omega \in \mathbb{B}_{m,1}^+ \cup \mathbb{B}_{m,1}^0 \\ \mu_0(\theta), & \text{if } \omega \in \mathbb{B}_{m,1}^- \end{cases} \quad (3.11)$$

2) If $\theta_m < \theta < \theta_c = q + 1$ then

$$P^\omega = \begin{cases} \mu_2(\theta, m), & \text{if } \omega \in \mathbb{B}_{m,1}^+ \\ \mu_1(\theta, m), & \text{if } \omega \in \mathbb{B}_{m,1}^0 \\ \mu_0(\theta), & \text{if } \omega \in \mathbb{B}_{m,1}^- \end{cases} \quad (3.12)$$

3) If $\theta = \theta_c$ then

$$P^\omega = \begin{cases} \mu_2(\theta, m), & \text{if } \omega \in \mathbb{B}_{m,0}^+ \\ \mu_0(\theta), & \text{if } \omega \in \mathbb{B}_{m,0}^- \cup \mathbb{B}_{m,0}^0 \end{cases} \quad (3.13)$$

4) If $\theta > \theta_c$ then

$$P^\omega = \begin{cases} \mu_2(\theta, m), & \text{if } \omega \in \mathbb{B}_{m,0}^+ \\ \mu_1(\theta, m), & \text{if } \omega \in \mathbb{B}_{m,0}^- \\ \mu_0(\theta), & \text{if } \omega \in \mathbb{B}_{m,0}^0 \end{cases} \quad (3.14)$$

For concrete examples of the boundary conditions mentioned in Theorem 3.7 see [29].

4. CONDITIONS OF (NON-) EXTREMALITY OF TISGMs

In this section we review results of papers [51], [110] about sufficient conditions for (non-)extremality of TISGMs of the Potts model, depending on coupling strength parameterized by θ , the block size m and the branch of the boundary law z .

Recall that by $\mu_i(\theta, m)$ we denote the TISGM which corresponds to the values of $z_i(\theta, m)$, $i = 1, 2$, which is a solution to (3.6).

Non-extremality.

Define the following numbers:

$$\widehat{\theta} = (\sqrt{2} - 1)q + 2m + 1, \quad \theta^* = 1 + (\sqrt{2} + 1)q - 2m. \quad (4.1)$$

Theorem 4.1. *Let $k = 2$, $2m < q$. Then the following statements hold.*

(i) *Assume one of the following conditions is satisfied:*

- a) $2 \leq m \leq q/7$ and $\theta \in [\theta_m, \widehat{\theta})$;
- b) $\theta \in (\theta^*, +\infty)$.

Then $\mu_1(\theta, m)$ is non-extreme.

(ii) *Assume one of the following conditions is satisfied:*

- c) $2 \leq m \leq q/7$ and $\theta \geq \theta_m$;
- d) $q < 7m$, $m \geq 2$ and $\theta \in (\widehat{\theta}, +\infty)$.

Then $\mu_2(\theta, m)$ is non-extreme. (See Fig.2-4)

Extremality. Denote $\theta_1 = 1 + 2\sqrt{q-1}$ and $\theta^* = 1 + (\sqrt{2} + 1)q - 2m$.

Theorem 4.2. *If $k = 2$, $m = 1$ then the following is true.*

(a) - *If $q = 3, 4, \dots, 16$ then there exists θ^{**} such that $\theta_c = q + 1 < \theta^{**} < \theta^*$ and the measure $\mu_1(\theta, 1)$ is extreme for any $\theta \in [\theta_1, \theta^{**})$. Moreover θ^{**} is the unique positive solution of the following equation*

$$\theta^3 - (q-3)\theta^2 - (2q-7)\theta - (q+5) = 0.$$

- *If $q \geq 17$ then there are $\bar{\theta}_1, \bar{\theta}_2 \in (\theta_1, \theta_c)$ such that $\bar{\theta}_1 < \bar{\theta}_2$ and the measure $\mu_1(\theta, 1)$ is extreme for any $\theta \in [\theta_1, \bar{\theta}_1) \cup (\bar{\theta}_2, \theta^{**})$. Moreover $\bar{\theta}_1, \bar{\theta}_2$ are positive solutions of the following equation*

$$\theta^3 - (q-1)\theta^2 - (2q-3)\theta + (4q^2 - 13q + 11) = 0.$$

(b) *The measure $\mu_2(\theta, 1)$ is extreme for any $\theta \geq \theta_1$, $q \geq 2$. (see Fig.5)*

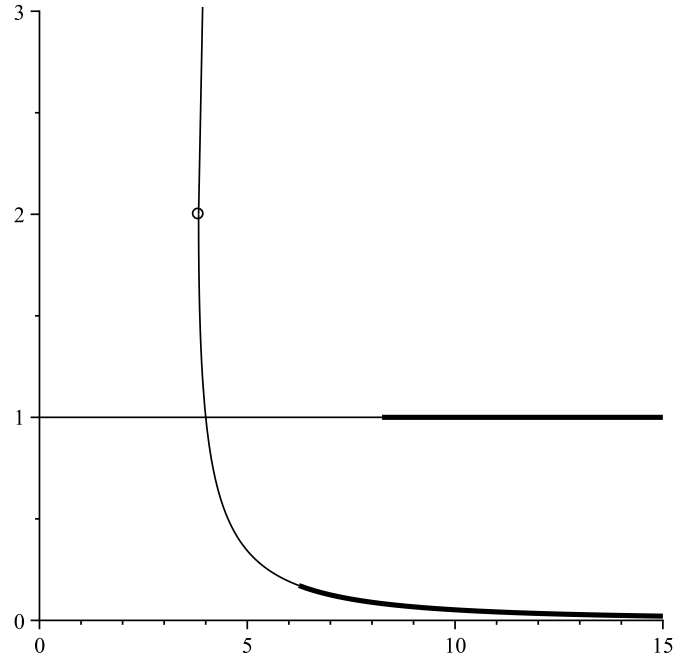


FIGURE 2. The graphs of the functions $z_i = z_i(m, \theta)$, $i = 1, 2$, for $q = 3$ and $m = 1$. The circle dot having coordinate $(\theta_1, 2)$ separates graph of z_1 from graph of z_2 . The bold curves correspond to regions of solutions where the corresponding TISGM is non-extreme. This figure corresponds to Part (i), b) of Theorem 4.1.

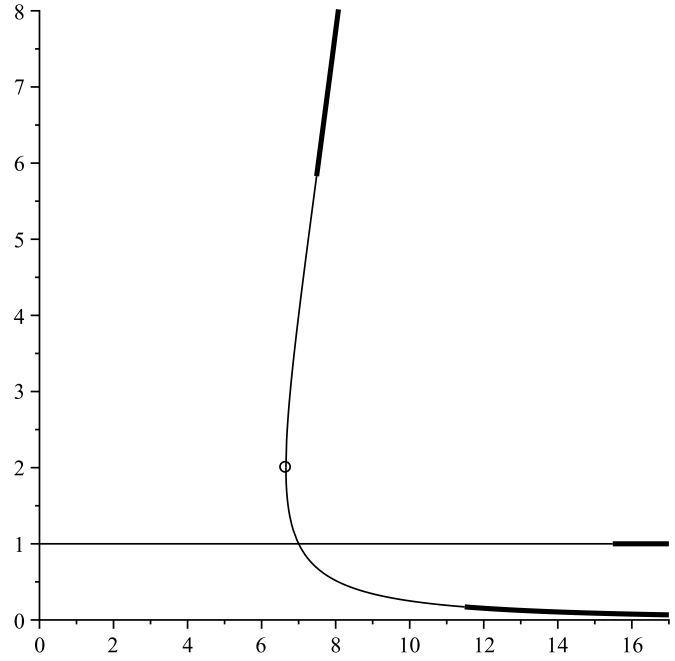


FIGURE 3. The graphs of the functions $z_i = z_i(m, \theta)$, $i = 1, 2$, for $q = 6$ and $m = 2$. The circle dot having coordinate $(\theta_2, 2)$ separates graph of z_1 from graph of z_2 . The bold lines correspond to regions of solutions where corresponding TISGM is non-extreme. The upper bold curve corresponds to part (ii), d) and the lower bold curve corresponds to part (i), b) of Theorem 4.1.

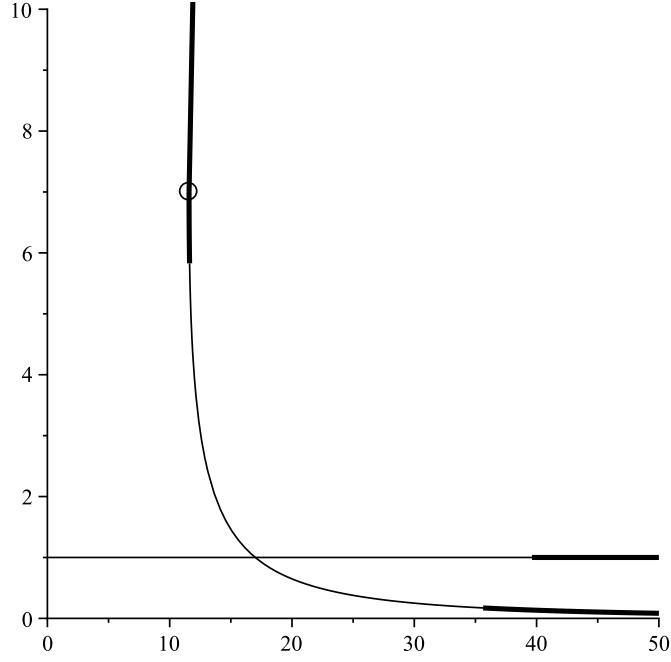


FIGURE 4. The graphs of the functions $z_i = z_i(m, \theta)$, $i = 1, 2$, for $q = 16$ and $m = 2$. The circle dot having coordinate $(\theta_2, 7)$ separates graph of z_1 from graph of z_2 . The bold lines correspond to regions of solutions where corresponding TISGM is non-extreme. The bold z_2 corresponds to Part (ii), c); Bold parts of z_1 correspond to Part (i), a) (upper bold curve) and Part (i), b) (lower bold curve) of Theorem 4.1.

The following theorem corresponds to the case: $m \geq 2$. From condition $2 \leq m \leq [q/2]$ it follows that $q \geq 4$.

Theorem 4.3. *Let $k = 2$.*

- (i) *If $m = 2$ then the following is true.*
- (i.1) *If $m = 2$ then for each $q = 4, 5, 6, 7, 8$ there exists $\check{\theta} > \theta_c = q + 1$ such that the measure $\mu_1(\theta, 2)$ is extreme for any $\theta \in [\theta_2, \check{\theta})$.*
- (i.2) *For each $q \geq 9$ there exists $\theta^\dagger \in (\theta_2, q + 1)$ such that the measure $\mu_1(\theta, 2)$ is extreme for any $\theta \in [\theta^\dagger, \check{\theta})$, where $\theta^\dagger = \theta^\dagger(q)$ is the unique solution of*

$$\theta^3 - (q + 3)\theta^2 + (6q - 17)\theta - (9q - 19) = 0$$

and $\check{\theta} = \check{\theta}(q)$ is the unique solution of

$$\theta^3 - (q + 3)\theta^2 - (2q - 15)\theta - (q + 13) = 0.$$

- (ii) *If $m = 2$ then for each $q = 4, 5, 6, 7, 8$ there exists $\hat{\theta} = \hat{\theta}(q)$ such that $\theta_2 < \hat{\theta} \leq q + 1$ and $\mu_2(\theta, 2)$ is extreme for $\theta \in [\theta_2, \hat{\theta})$ (see Fig.6).*
- (iii) *If $q < \frac{m+1}{2m} [3m + 1 + \sqrt{m^2 + 6m + 1}]$ and $m \geq 2$ then the measure $\mu_1(\theta_m, m) = \mu_2(\theta_m, m)$ is extreme.*

Now following [110] we give a theorem which is more general than Theorem 4.3.

Theorem 4.4. *Let $k = 2$, $m \geq 2$. Then*

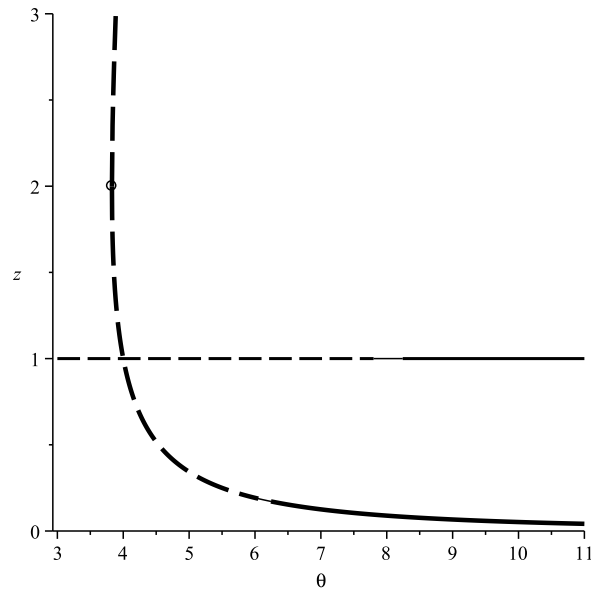


FIGURE 5. The graphs of the functions $z_i = z_i(m, \theta)$, for $q = 3$, $m = 1$ and the graph of $z(\theta) \equiv 1$. The bold curves correspond to regions of solutions where the corresponding TISGM is non-extreme (corresponds to part (ii), b) of Theorem 4.1). The dashed bold curves correspond to regions of solutions where the corresponding TISGM is extreme (see parts (a) and (b) of Theorem 4.2). The gaps between the two types of curves are given by thin curves.

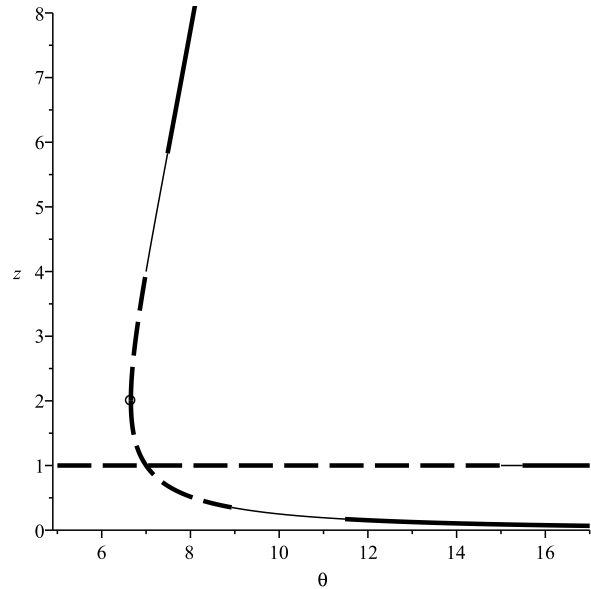


FIGURE 6. The graphs of the functions $z_i = z_i(m, \theta)$, for $q = 6$, $m = 2$ and the graph of $z(\theta) \equiv 1$. The types of curves corresponding to certain extremality and certain non-extremality are as in Fig.5 (corresponds to Theorem 4.3).

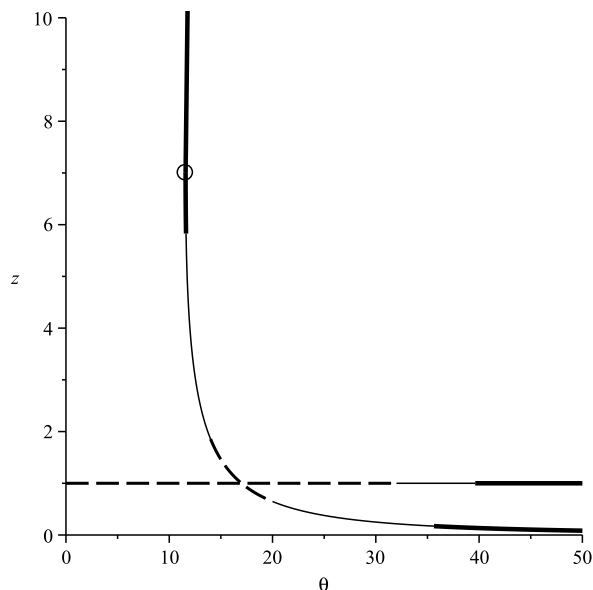


FIGURE 7. The graphs of the functions $z_i = z_i(m, \theta)$, for $q = 16$, $m = 2$ and the graph of $z(\theta) \equiv 1$. The types of curves are again as in Fig.5 (corresponds to part a) of Theorem 4.5).

1. If $2m \leq q < \frac{m+1}{2m}[3m+1 + \sqrt{m^2 + 6m + 1}]$, then there is $\bar{\theta} > q+1$ such that the measure $\mu_1(\theta, m)$ is extreme for any $\theta \in [\theta_m, \bar{\theta})$;
2. If $q > \frac{m+1}{2m}[3m+1 + \sqrt{m^2 + 6m + 1}]$, then there exists $\bar{\theta} \in (\theta_m, \theta_c)$ such that the measure $\mu_1(\theta, m)$ is extreme for any $\theta \in (\bar{\theta}, \bar{\theta})$;
3. If $2m \leq q < m + \frac{1}{4m}(m+1 + \sqrt{m^2 + 2m + 7})^2$ there is $\bar{\theta} \in (\theta_m, +\infty)$ such that the measure $\mu_2(\theta, m)$ is extreme for any $\theta \in [\theta_m, \bar{\theta})$.

Remark 4.1. Note that

- If $q > m + \frac{1}{4m}(m+1 + \sqrt{m^2 + 2m + 7})^2$, then it is unknown whether the measure $\mu_2(\theta, m)$ is extreme in this case.
- In [110] for the 3-state Potts model on the Cayley tree of order $k = 3$, the extremality questions are studied for certain TISGMs. The case $k \geq 4$ is not considered yet. Because in this case there is not explicit formula of nontrivial solutions to the equation (3.6).

Now we give results which are valid for θ close to the critical value θ_c at which the lower branches of the boundary law z degenerate into the free value $z = 1$ and the corresponding Markov chains become close to the free chain.

Theorem 4.5. *Let $k = 2$.*

- a) For each $m \leq [q/2]$ there exists a neighborhood $U_m(\theta_c)$ of θ_c such that the measure $\mu_1(\theta, m)$ is extreme if $\theta \in U_m(\theta_c)$ (see Fig.7).
- b) If $m = 1$ or condition (iii) of Theorem 4.3 is satisfied then there exists a neighborhood $V_m(\theta_m)$ of θ_m such that measures $\mu_i(\theta, m)$, $i = 1, 2$ are extreme if $\theta \in V_m(\theta_m)$.

Recall that the model is called ferromagnetic if $\theta > 1$, and as usual a punctured neighborhood of θ_c is an open neighborhood from which the value θ_c was removed.

Theorem 4.6. *For the ferromagnetic q -state Potts model (with $q \geq 3$) on the Cayley tree of order two, there exists a punctured neighborhood $U(\theta_c)$ of θ_c such that there are at least $2^{q-1} + q$ extreme TISGMs for each $\theta \in U(\theta_c)$.*

5. TISGMs IN CASE OF A NON-ZERO EXTERNAL FIELD

This section is devoted to review results of [10] concerning TISGMs in case of a non-zero external field.

For simplicity, in (2.3) we choose the external field such that all coordinates of the (reduced) vector $\check{\xi}^0$ (see Remark 2.1) are zero except one; due to permutational symmetry, we may assume, without loss of generality, that $\check{\xi}_1^0 = \alpha \in \mathbb{R}$ and $\check{\xi}_2^0 = \dots = \check{\xi}_{q-1}^0 = 0$,

$$\check{\xi}^0 = (\alpha, 0, \dots, 0) \in \mathbb{R}^{q-1}. \quad (5.1)$$

We also write

$$\check{h}^0 = (\check{h}_1^0, \dots, \check{h}_{q-1}^0) \in \mathbb{R}^{q-1}.$$

Then, denoting $z_i := \theta^{\check{h}_i^0/k}$ ($i = 1, \dots, q-1$), the compatibility equations (3.2) are equivalently rewritten in the form

$$\begin{cases} z_1 = 1 + \frac{(\theta - 1)(\theta^\alpha z_1^k - 1)}{\theta + \theta^\alpha z_1^k + \sum_{j=2}^{q-1} z_j^k}, \\ z_i = 1 + \frac{(\theta - 1)(z_i^k - 1)}{\theta + \theta^\alpha z_1^k + \sum_{j=2}^{q-1} z_j^k}, \quad i = 2, \dots, q-1. \end{cases} \quad (5.2)$$

Assume $\alpha \neq 0$. The system (5.2) with $\theta > 1$ is reduced either to a single equation

$$u = 1 + \frac{(\theta - 1)(\theta^\alpha u^k - 1)}{\theta + \theta^\alpha u^k + q - 2} \quad (5.3)$$

or to the system of equations (indexed by $m = 1, \dots, q-2$)

$$\begin{cases} u = 1 + \frac{(\theta - 1)(\theta^\alpha u^k - 1)}{\theta + \theta^\alpha u^k + mv^k + q - 2 - m}, \\ 1 = \frac{(\theta - 1)(1 + v + \dots + v^{k-1})}{\theta + \theta^\alpha u^k + mv^k + q - 2 - m}, \\ v \neq 1. \end{cases} \quad (5.4)$$

To give the solvability of the equation (5.3) let us introduce some notations. Denote

$$\theta_c = \theta_c(k, q) := \frac{1}{2} \left(\sqrt{(q-2)^2 + 4(q-1) \left(\frac{k+1}{k-1} \right)^2} - (q-2) \right). \quad (5.5)$$

$$b = b(\theta) := \frac{\theta(\theta + q - 2)}{q - 1}. \quad (5.6)$$

For $\theta \geq \theta_c$, denote by $x_\pm = x_\pm(\theta)$ the roots of the quadratic equation

$$(b+x)(1+x) = k(b-1)x \quad (5.7)$$

with discriminant

$$D = D(\theta) := (k(b-1) - (b+1))^2 - 4b = (b-1)(k-1)^2 \left(b - \left(\frac{k+1}{k-1} \right)^2 \right), \quad (5.8)$$

that is,

$$x_{\pm} = x_{\pm}(\theta) := \frac{(b-1)(k-1) - 2 \pm \sqrt{D}}{2}. \quad (5.9)$$

Introduce the following notations

$$a_{\pm} = a_{\pm}(\theta) := \frac{1}{x_{\pm}} \left(\frac{1+x_{\pm}}{b+x_{\pm}} \right)^k, \quad \theta \geq \theta_c. \quad (5.10)$$

$$\alpha_{\pm} = \alpha_{\pm}(\theta) := -(k+1) + \frac{1}{\ln \theta} \ln \frac{q-1}{a_{\mp}}, \quad \theta \geq \theta_c, \quad (5.11)$$

so that $\alpha_-(\theta_c) = \alpha_+(\theta_c)$ and $\alpha_-(\theta) < \alpha_+(\theta)$ for $\theta > \theta_c$.

Theorem 5.1. *Let $\nu_0(\theta, \alpha)$ denote the number of TISGMs corresponding to the solutions $u > 0$ of the equation (5.3). Then*

$$\nu_0(\theta, \alpha) = \begin{cases} 1 & \text{if } \theta \leq \theta_c \text{ or } \theta > \theta_c \text{ and } \alpha \notin [\alpha_-, \alpha_+], \\ 2 & \text{if } \theta > \theta_c \text{ and } \alpha \in \{\alpha_-, \alpha_+\}, \\ 3 & \text{if } \theta > \theta_c \text{ and } \alpha \in (\alpha_-, \alpha_+), \end{cases}$$

where θ_c is given in (5.5) and $\alpha_{\pm} = \alpha_{\pm}(\theta)$ are defined by (5.11).

Consider now the set of equations (5.4). For each $m \in \{1, \dots, q-2\}$, consider the functions

$$L_m(v; \theta) := (\theta - 1)(v^{k-1} + \dots + v) - mv^k - (q-1-m), \quad (5.12)$$

$$K_m(v; \theta) := \frac{(v^{k-1} + \dots + v + 1)^k L_m(v; \theta)}{(v^{k-1} + \dots + v + L_m(v; \theta))^k}. \quad (5.13)$$

For any $\theta > 1$ there is a unique value $v_m = v_m(\theta) > 0$ such that

$$L_m^*(\theta) := L_m(v_m; \theta) = \max_{v>0} L_m(v; \theta).$$

Moreover, the function $\theta \mapsto L_m^*(\theta)$ is strictly increasing. Denote by θ_m the unique value of $\theta > 1$ such that

$$L_m^*(\theta_m) = 0. \quad (5.14)$$

Thus, for any $\theta > \theta_m$ the range of the functions $v \mapsto L_m(v; \theta)$ and $v \mapsto K_m(v; \theta)$ includes positive values,

$$\mathcal{V}_m^+(\theta) := \{v > 0: L_m(v; \theta) > 0\} \equiv \{v > 0: K_m(v; \theta) > 0\} \neq \emptyset, \quad (5.15)$$

and, therefore, the function

$$\alpha_m(\theta) := \frac{1}{\ln \theta} \max_{v \in \mathcal{V}_m^+(\theta)} \ln K_m(v; \theta) = \frac{\ln K_m^*(\theta)}{\ln \theta}, \quad \theta > \theta_m, \quad (5.16)$$

is well defined, where

$$K_m^*(\theta) := \max_{v \in \mathcal{V}_m^+(\theta)} K_m(v; \theta).$$

Theorem 5.2. *For each $m \in \{1, \dots, q-2\}$, let $\nu_m(\theta, \alpha)$ denote the number of TISGMs corresponding to positive solutions (u, v) of the system (5.4). Then $\nu_m(\theta, \alpha) \geq 1$ if and only if $\theta > \theta_m$ and $\alpha \leq \alpha_m(\theta)$.*

In the case $q = 3$, there is an additional critical value

$$\tilde{\theta}_1 = \tilde{\theta}_1(k) := \frac{5 - k + \sqrt{49k^2 + 62k + 49}}{6(k - 1)}. \quad (5.17)$$

For $q \geq 2$, consider the following subsets of the half-plane

$$\{\theta \geq 1\} = \{(\theta, \alpha) : \theta \geq 1, \alpha \in \mathbb{R}\}.$$

$$A_q := \{\theta > \theta_c, \alpha_-(\theta) \leq \alpha \leq \alpha_+(\theta)\},$$

$$B_q := \begin{cases} \emptyset & \text{if } q = 2, \\ \{\theta > \theta_1, \alpha < \alpha_1(\theta)\} \cup \{\theta > \tilde{\theta}_1, \alpha = \alpha_1(\theta)\} & \text{if } q = 3, \\ \{\theta > \theta_1, \alpha \leq \alpha_1(\theta)\} & \text{if } q \geq 4. \end{cases} \quad (5.18)$$

Denote the total number of TISGMs corresponding to positive solutions $\mathbf{z} = (z_1, \dots, z_{q-1})$ of the system of equations (5.2) by $\nu(\theta, \alpha)$ where $\theta \geq 1$, $\alpha \in \mathbb{R}$ (of course, this number also depends on k and q). Theorems 5.1 and 5.2 is summarized as follows.

Theorem 5.3 (Non-uniqueness).

- (a) If $q = 2$ then $\nu(\theta, \alpha) \geq 2$ if and only if $(\theta, \alpha) \in A_2 \cup B_2 = A_2$.
- (b) If $q = 3$ then $\nu(\theta, \alpha) \geq 2$ if $(\theta, \alpha) \in A_3 \cup B_3$. The “only if” statement holds true at least for $k = 2, 3, 4$.
- (c) If $q \geq 4$ then $\nu(\theta, \alpha) \geq 2$ if and only if $(\theta, \alpha) \in A_q \cup B_q$.

Theorem 5.3 provides a sufficient and (almost) necessary condition for the uniqueness of solution of (5.2), illustrated in Figure 8 for $q = 5$ and $q = 3$, both with $k = 2$.

To conclude this subsection, the following result describes a few cases where it is possible to estimate the maximal number of solutions of the system (5.2).

Theorem 5.4.

- (a) If $q = 2$ then $\nu(\theta, \alpha) \leq 3$; moreover, $\nu(\theta, \alpha) = 3$ for all $\theta \geq 1$ large enough.
- (b) Let $\alpha = 0$ and $k \geq 2$. Then $\nu(\theta, 0) \leq 2^q - 1$ for all $\theta \geq 1$; moreover, $\nu(\theta, 0) = 2^q - 1$ for all θ large enough.
- (c) If $k = 2$ then $\nu(\theta, \alpha) \leq 2^q - 1$ for all $\theta \geq 1$ and $\alpha \in \mathbb{R}$.

The general case $q \geq 3$ with $\alpha \in \mathbb{R}$ was first addressed by Peruggi et al. [81] (and continued in [82]) using physical argumentation. In particular, they correctly identified the critical point θ_c [82, equation (22), page 160] (cf. (5.5)) and also suggested an explicit critical boundary in the phase diagram for $\alpha \geq 0$, defined by the expression [82, equation (21), page 160]:

$$\tilde{\alpha}_-(\theta) = \frac{(k + 1) \ln(1 + (q - 2)/\theta) - (k - 1) \ln(q - 1)}{2 \ln \theta}.$$

6. PERIODIC SGMS

6.1. Definitions. Let $\Gamma^k = (V, L)$ be a Cayley tree of order $k \geq 2$.

Consider q -state Potts model with an external field:

$$H(\sigma) = -J \sum_{\langle x, y \rangle \in L} \delta_{\sigma(x)\sigma(y)} - \alpha \sum_{x \in V} \delta_{1\sigma(x)} \quad (6.1)$$

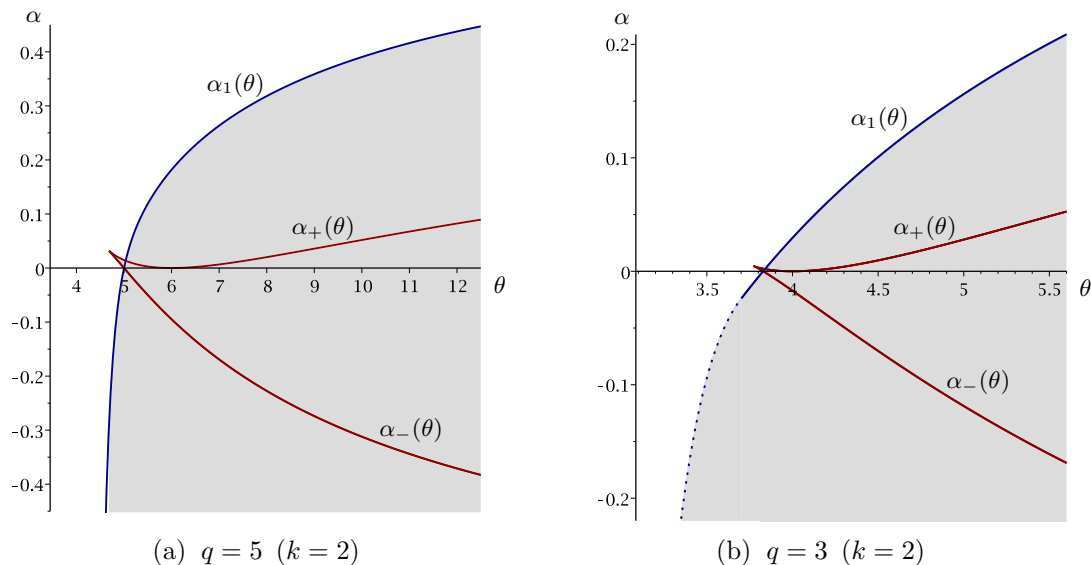


FIGURE 8. The phase diagram for the Potts model (5.1) showing the non-uniqueness region (shaded in grey) according to Theorem 5.3: (a) regular case $q \geq 4$ (shown here for $q = 5$); (b) special case $q = 3$, both with $k = 2$. The critical boundaries are determined by (parts of) the graphs of the functions $\alpha_{\pm}(\theta)$ and $\alpha_1(\theta)$ defined in (5.11) and (5.16), respectively. The dotted part of the boundary on panel (b), given by $\alpha = \alpha_1(\theta)$, $\theta \in (\theta_1, \tilde{\theta}_1]$ (see formula (5.18) with $q = 3$), is excluded from the shaded region (see Theorem 5.3(b); here, $\theta_1 = 3$ and $\tilde{\theta}_1 = \frac{1}{2}(1 + \sqrt{41}) \doteq 3.7016$).

where $J, \alpha \in \mathbb{R}$.

By Theorem 2.1 we have that to each splitting Gibbs measures of this model corresponds a set of vectors $h_x \in \mathbb{R}^{q-1}$, $x \in V$ which satisfies

$$h_x = \sum_{y \in S(x)} F(h_y, \theta, \alpha), \quad (6.2)$$

where $F : h = (h_1, \dots, h_{q-1}) \in \mathbb{R}^{q-1} \rightarrow F(h, \theta, \alpha) = (F_1, \dots, F_{q-1}) \in \mathbb{R}^{q-1}$ defined as:

$$F_i = \alpha\beta\delta_{1i} + \ln \left(\frac{(\theta - 1)e^{h_i} + \sum_{j=1}^{q-1} e^{h_j} + 1}{\theta + \sum_{j=1}^{q-1} e^{h_j}} \right),$$

$\theta = \exp(J\beta)$, and $S(x)$ is the set of all direct successors of $x \in V$ (see (2.2)).

Recall G_k is the group which represents the Cayley tree (see Section 2). Let $G_k/G_k^* = \{H_1, \dots, H_r\}$ be the quotient group, where G_k^* is a normal subgroup of index $r \geq 1$.

Definition 6.1. A set of vectors $h = \{h_x, x \in G_k\}$ is said to be G_k^* -periodic, if $h_{yx} = h_x$ for any $x \in G_k$ and $y \in G_k^*$. A G_k -periodic set is called translation-invariant.

Definition 6.2. A set of vectors $h = \{h_x, x \in G_k\}$ is said to be G_k^* -weakly periodic, if $h_x = h_{ij}$ for $x \in H_i$ and $x_{\downarrow} \in H_j$ for any $x \in G_k$.

Definition 6.3. A measure μ is said to be G_k^* -periodic (weakly periodic), if it corresponds to the G_k^* -periodic (weakly periodic) set of vectors h . The G_k -periodic measure is said to be translation-invariant.

In this section we review the results of [45]-[48], [104], [87]-[91] related to (weakly) periodic Gibbs measures of the Potts model.

Let $G_k^{(2)}$ be the subgroup in G_k consisting of all words of even length. Clearly, $G_k^{(2)}$ is a subgroup of index 2.

The following theorem characterizes all periodic Gibbs measures.

Theorem 6.1. *Let K be a normal subgroup of finite index in G_k . Then each K -periodic Gibbs measure for the Potts model (6.1) is either translation-invariant or $G_2^{(2)}$ -periodic.*

Since TISGMs are given in previous sections, by Theorem 6.1 it suffices consider $G_k^{(2)}$ -periodic Gibbs measure only. Such measures correspond to the set of vectors $h = \{h_x \in \mathbb{R}^{q-1} : x \in G_k\}$ of the form

$$h_x = \begin{cases} \mathbf{h}^1, & \text{if } |x| \text{ is even,} \\ \mathbf{h}^2, & \text{if } |x| \text{ is odd,} \end{cases}$$

where $|x|$ denotes the length of the word x and the vectors $\mathbf{h}^1 = (h_1, h_2, \dots, h_{q-1})$, $\mathbf{h}^2 = (l_1, l_2, \dots, l_{q-1})$, by (6.2), should satisfy

$$\begin{cases} h_i = k \ln \frac{(\theta - 1) \exp(l_i) + \sum_{j=1}^{q-1} \exp(l_j) + 1}{\sum_{j=1}^{q-1} \exp(l_j) + \theta}, \\ l_i = k \ln \frac{(\theta - 1) \exp(h_i) + \sum_{j=1}^{q-1} \exp(h_j) + 1}{\sum_{j=1}^{q-1} \exp(h_j) + \theta} \end{cases} \quad i = 1, \dots, q-1.$$

Denoting $\exp(h_i) = x_i$, $\exp(l_i) = y_i$ the last system can be written as

$$\begin{aligned} x_i &= \left(\frac{(\theta - 1)y_i + \sum_{j=1}^{q-1} y_j + 1}{\sum_{j=1}^{q-1} y_j + \theta} \right)^k, \\ y_i &= \left(\frac{(\theta - 1)x_i + \sum_{j=1}^{q-1} x_j + 1}{\sum_{j=1}^{q-1} x_j + \theta} \right)^k \end{aligned} \quad i = 1, \dots, q-1. \quad (6.3)$$

Consider mapping $W : \mathbb{R}_+^{q-1} \times \mathbb{R}_+^{q-1} \rightarrow \mathbb{R}_+^{q-1} \times \mathbb{R}_+^{q-1}$, defined by

$$\begin{aligned} x'_i &= \left(\frac{(\theta - 1)y_i + \sum_{j=1}^{q-1} y_j + 1}{\sum_{j=1}^{q-1} y_j + \theta} \right)^k, \\ y'_i &= \left(\frac{(\theta - 1)x_i + \sum_{j=1}^{q-1} x_j + 1}{\sum_{j=1}^{q-1} x_j + \theta} \right)^k \end{aligned} \quad i = 1, \dots, q-1. \quad (6.4)$$

Note that (6.3) is the equation $z = W(z)$, with

$$z = (x_1, \dots, x_{q-1}, y_1, \dots, y_{q-1})$$

that is equation for fixed points of the mapping W .

For $m \leq q - 1$ introduce the set

$$I_m = \{x = (x_1, \dots, x_{q-1}) \in \mathbb{R}_+^{q-1} : x_1 = \dots = x_m, \quad x_{m+1} = \dots = x_{q-1} = 1\}.$$

Let S_{q-1} be the group of permutations on $\{1, \dots, q - 1\}$.

For $\pi = (\pi(1), \dots, \pi(q - 1)) \in S_{q-1}$ and $x \in \mathbb{R}^{q-1}$ define

$$\pi x = (x_{\pi(1)}, \dots, x_{\pi(q-1)}),$$

and for a subset $I \subset \mathbb{R}^{q-1}$ define

$$\pi I = \{\pi x : x \in I\}.$$

The following lemma is useful to find special solutions of (6.3).

Lemma 6.2. *For any $\pi \in S_{q-1}$ and $m \leq q - 1$ the set $\pi I_m \times \pi I_m$ is invariant with respect to the mapping W .*

6.2. Zero external field. In this section consider the case $\alpha = 0$.

Ferromagnetic case. In [47], it is shown that in the ferromagnetic case (i.e. $J > 0$) each periodic measure is translation-invariant:

Theorem 6.3. *Let $k \geq 2$, $q \geq 2$, $J > 0$, $\alpha = 0$. Then any periodic Gibbs measure of the model (6.1) is translation-invariant.*

For $q = 3$ this theorem was proved in [104].

Anti-ferromagnetic case. Note that the case $q = 2$ corresponds to anti-ferromagnetic Ising model, which has periodic measures for any $k \geq 2$ ([36], [103]).

In this subsection we consider the anti-ferromagnetic case (i.e. $J < 0$) and review results of [46], [48] and [47] that for $k = 2$, $q \geq 3$ there is no periodic (except translation-invariant) Gibbs measures. But for $k \geq 3$, $q \geq 2$ there are several periodic (non-translation-invariant) Gibbs measures.

Theorem 6.4. *Let $k = 2$, $q \geq 3$, $J < 0$, and $\alpha = 0$. Then the $G_k^{(2)}$ -periodic Gibbs measure for the Potts model is unique. Moreover, this measure coincides with the unique translation-invariant Gibbs measure.*

In case $k \geq 3$, we have the following

Theorem 6.5. *Let $k \geq 3$, $q \geq 3$, $J < 0$ and $\theta_{cr} = \frac{k-q+1}{k+1}$. Then for the Potts model for $0 < \theta < \theta_{cr}$ there are exactly three $G_k^{(2)}$ -periodic Gibbs measures, corresponding to solutions on $I_m \times I_m$. Moreover, only one of these measures is translation-invariant.*

Using symmetry of solutions, one obtains the following:

Theorem 6.6. *For the Potts model on the Cayley tree of order $k \geq 3$, if $3 \leq q < k+1$ and $0 < \theta < \theta_{cr}$ then the number of $G_k^{(2)}$ -periodic Gibbs measures is at least $2 \cdot (2^q - 1)$.*

6.3. Non-zero external field. In case $\alpha \neq 0$, the system of equations for periodic solutions becomes more complicated to solve. Because in this case the symmetry of solutions will be lost.

In this subsection following [104] we consider a particular case of parameters and give a result that under some conditions on parameters the model has periodic (non-translation-invariant) Gibbs measures.

Let $k = 2$, $q = 3$ and $e^{\alpha\beta} = \lambda$, where $\alpha \in \mathbb{R}$ is the external field, and as before, $\beta = \frac{1}{T}$, $T > 0$.

Periodic measures correspond to positive solutions of

$$\begin{cases} x = \zeta \cdot \frac{\theta y^2 + 2}{y^2 + \theta + 1} \\ y = \zeta \cdot \frac{\theta x^2 + 2}{x^2 + \theta + 1} \end{cases} \quad (6.5)$$

where $\zeta = \sqrt{\lambda}$.

This system, in case $x = y$, can be written as

$$x^3 - \zeta\theta x^2 + (\theta + 1)x - 2\zeta = 0, \quad (6.6)$$

which gives translation-invariant measures.

Substituting the expression for y from the second equation in the first equation, we obtain a fifth-degree equation in x . Dividing the fifth-degree polynomial from the obtained equation by the third-degree polynomial from (6.6), we obtain the quadratic equation

$$(\zeta^2\theta^2 + \theta + 1)x^2 + (-2\zeta + \zeta\theta(\theta + 1))x + 2\zeta^2\theta + (\theta + 1)^2 = 0, \quad (6.7)$$

which describes periodic Gibbs measures. We now study solutions of this quadratic equation. For this, we calculate its discriminant taking into account that $\sqrt{\lambda} = \zeta$:

$$D = -8\theta^3\lambda^2 - [3\theta^2(\theta + 1)^2 + 12\theta(\theta + 1) - 4]\lambda - 4(\theta + 1)^3.$$

It is known that equation (6.7) has two positive real roots if $D > 0$ and if $-2\zeta + \zeta\theta(\theta + 1) = \zeta(\theta^2 + \theta - 2) < 0$. Solving these inequalities, we find that equation (6.7) has two real solutions if $0 < \theta < \frac{\sqrt{17}-3}{6} = \theta^*$ and $\lambda_1(\theta) < \lambda < \lambda_2(\theta)$, where $\lambda_1(\theta)$, $\lambda_2(\theta)$ has the following form

$$\begin{aligned} \lambda_1(\theta) &= \frac{-3[3\theta^2(\theta + 1)^2 + 12\theta(\theta + 1) - 4] - (\theta - 1)(\theta + 2)\sqrt{K}}{48\theta^3}, \\ \lambda_2(\theta) &= \frac{-3[3\theta^2(\theta + 1)^2 + 12\theta(\theta + 1) - 4] + (\theta - 1)(\theta + 2)\sqrt{K}}{48\theta^3}, \end{aligned} \quad (6.8)$$

where

$$K = (\theta - 1)(\theta + 2)(9\theta^2 + 9\theta - 2).$$

Note that for $0 < \theta < \theta^*$ both $\lambda_1(\theta)$ and $\lambda_2(\theta)$ are positive.

If $\theta^* < \theta < 1$, then equation (6.7) has no real solutions. Moreover, equation (6.7) also has no real solutions for $\theta > 1$.

Let now $\theta = \theta^*$. Then for $\lambda = \lambda^*$, where

$$\lambda^* = -\frac{3(\theta^*)^2(\theta^* + 1)^2 + 12\theta^*(\theta^* + 1) - 4}{16(\theta^*)^3}, \quad (6.9)$$

the discriminant of the equation (6.7) is $D = 0$. Consequently, the equation (6.7) has unique solution:

$$x^* = \frac{\zeta^*(2 - \theta^* - (\theta^*)^2)}{2((\zeta^*)^2(\theta^*)^2 + \theta^* + 1)},$$

where $\zeta^* = \sqrt{\lambda^*}$.

Thus we have the following theorem:

Theorem 6.7. *For the Potts model, in case $k = 2$, $q = 3$, $\alpha \neq 0$ we have*

1. *If $\lambda \in (\lambda_1(\theta), \lambda_2(\theta))$ and $\theta \in (0, \theta^*)$, then there are at least two $G_k^{(2)}$ -periodic (non-translation-invariant) Gibbs measures, where $\theta^* = \frac{\sqrt{17}-3}{6}$, and λ_1, λ_2 defined by (6.8);*
2. *For $\lambda = \lambda^*$ and $\theta = \theta^*$, there are at least one $G_k^{(2)}$ -periodic (non-translation-invariant) Gibbs measure, where λ^* is defined in (6.9);*

7. WEAKLY PERIODIC MEASURES.

In this section following [87]-[90] we give some weakly periodic Gibbs measures (see Definition 6.3) of the Potts model.

The level of difficulty in describing of weakly periodic Gibbs measures is related to the structure and index of the normal subgroup relative to which the periodicity condition is imposed.

From Chapter 1 of [103] (see also [59]) we know that in the group G_k , there is no normal subgroup of odd index different from one. Therefore, we consider normal subgroups of even indices. In this section we restrict ourself to the case of indices two.

It is known (see [34] and [103]) that any normal subgroup of index two of the group G_k has the form

$$H_A = \left\{ x \in G_k : \sum_{i \in A} \omega_x(a_i) \text{--even} \right\},$$

where $\emptyset \neq A \subseteq N_k = \{1, 2, \dots, k+1\}$, and $\omega_x(a_i)$ is the number of letters a_i in a word $x \in G_k$.

Let $A \subseteq N_k$ and H_A be the corresponding normal subgroup of index two. We note that in the case $|A| = k+1$, i.e., in the case $A = N_k$, weak periodicity coincides with ordinary periodicity.

Consider $G_k/H_A = \{H_A, G_k \setminus H_A\}$ the quotient group.

For simplicity of notations, we denote $H_0 = H_A$, $H_1 = G_k \setminus H_A$.

The H_0 -weakly periodic collections of vectors $h = \{h_x \in \mathbb{R}^{q-1} : x \in G_k\}$ have the form:

$$h_x = \begin{cases} h_1, & \text{if } x_\downarrow \in H_0, x \in H_0 \\ h_2, & \text{if } x_\downarrow \in H_0, x \in H_1 \\ h_3, & \text{if } x_\downarrow \in H_1, x \in H_0 \\ h_4, & \text{if } x_\downarrow \in H_1, x \in H_1. \end{cases} \quad (7.1)$$

Here $h_i = (h_{i1}, h_{i2}, \dots, h_{iq-1})$, $i = 1, 2, 3, 4$.

Remark 7.1. The definition of x_\downarrow depends on the (fixed) root e of the Cayley tree. Therefore the function h_x given in (7.1) is defined for $x \neq e$.

By (6.2) we then have

$$\begin{cases} h_1 = (k - |A|)F(h_1, \theta, \alpha) + |A|F(h_2, \theta, \alpha) \\ h_2 = (|A| - 1)F(h_3, \theta, \alpha) + (k + 1 - |A|)F(h_4, \theta, \alpha) \\ h_3 = (|A| - 1)F(h_2, \theta, \alpha) + (k + 1 - |A|)F(h_1, \theta, \alpha) \\ h_4 = (k - |A|)F(h_4, \theta, \alpha) + |A|F(h_3, \theta, \alpha). \end{cases} \quad (7.2)$$

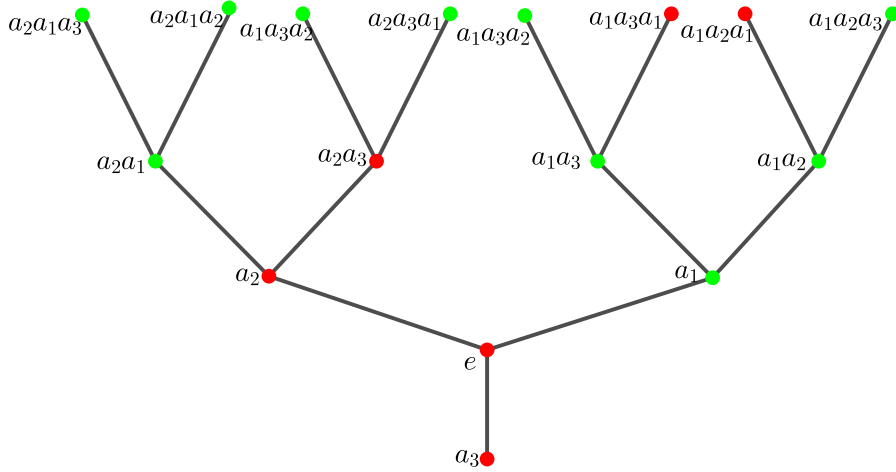


FIGURE 9. Partition (red and green) of the Cayley tree with respect to subgroup $H_{\{1\}}$ of index two.

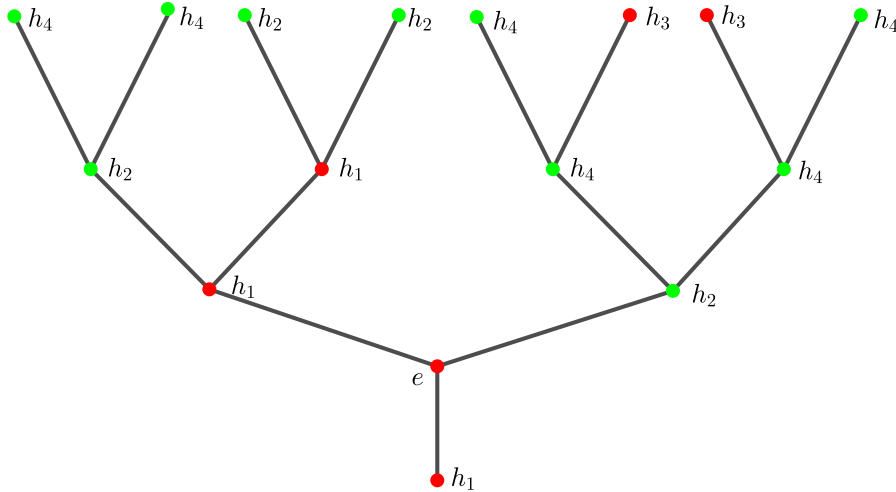


FIGURE 10. The values of the weakly-periodic function (7.1) in case $A = \{1\}$, i.e. subgroup $H_{\{1\}}$ of index two.

Let us give an examples geometrically presenting the vector-values of h_x on the Cayley tree.

Example 7.1. Let $A = \{1\}$. Then

$$H_A = H_{\{1\}} = \{x \in G_k : \text{number of } a_1 \text{ in } x \text{ is even}\},$$

In this case $H_0 = H_{\{1\}}$ (red points in Fig. 9) and $H_1 = G_k \setminus H_0$ is the set of words with an odd number of a_1 (green points in the Fig. 9).

In the Fig.10 we showed the distribution of the four values of function (7.1).

Denote $z_{ij} = \exp h_{ij}$, $\lambda_j = \exp(\alpha_j)$, $i = 1, 2, 3, 4$, $j = 1, 2, \dots, q-1$. Then the last system of equations can be rewritten as

$$\begin{cases} z_{1j} = \lambda_j \left(\frac{(\theta-1)z_{1j} + \sum_{i=1}^{q-1} z_{1i} + 1}{\sum_{i=1}^{q-1} z_{1i} + \theta} \right)^{k-|A|} \left(\frac{(\theta-1)z_{2j} + \sum_{i=1}^{q-1} z_{2i} + 1}{\sum_{i=1}^{q-1} z_{2i} + \theta} \right)^{|A|} \\ z_{2j} = \lambda_j \left(\frac{(\theta-1)z_{3j} + \sum_{i=1}^{q-1} z_{3i} + 1}{\sum_{i=1}^{q-1} z_{3i} + \theta} \right)^{|A|-1} \left(\frac{(\theta-1)z_{4j} + \sum_{i=1}^{q-1} z_{4i} + 1}{\sum_{i=1}^{q-1} z_{4i} + \theta} \right)^{k+1-|A|} \\ z_{3j} = \lambda_j \left(\frac{(\theta-1)z_{2j} + \sum_{i=1}^{q-1} z_{2i} + 1}{\sum_{i=1}^{q-1} z_{2i} + \theta} \right)^{|A|-1} \left(\frac{(\theta-1)z_{1j} + \sum_{i=1}^{q-1} z_{1i} + 1}{\sum_{i=1}^{q-1} z_{1i} + \theta} \right)^{k+1-|A|} \\ z_{4j} = \lambda_j \left(\frac{(\theta-1)z_{4j} + \sum_{i=1}^{q-1} z_{4i} + 1}{\sum_{i=1}^{q-1} z_{4i} + \theta} \right)^{k-|A|} \left(\frac{(\theta-1)z_{3j} + \sum_{i=1}^{q-1} z_{3i} + 1}{\sum_{i=1}^{q-1} z_{3i} + \theta} \right)^{|A|}, \end{cases} \quad (7.3)$$

here $j = 1, 2, 3, \dots, q-1$.

Define the map $K : \mathbb{R}^{4(q-1)} \rightarrow \mathbb{R}^{4(q-1)}$, as

$$\begin{cases} z'_{1j} = \lambda_j \left(\frac{(\theta-1)z_{1j} + \sum_{i=1}^{q-1} z_{1i} + 1}{\sum_{i=1}^{q-1} z_{1i} + \theta} \right)^{k-|A|} \left(\frac{(\theta-1)z_{2j} + \sum_{i=1}^{q-1} z_{2i} + 1}{\sum_{i=1}^{q-1} z_{2i} + \theta} \right)^{|A|} \\ z'_{2j} = \lambda_j \left(\frac{(\theta-1)z_{3j} + \sum_{i=1}^{q-1} z_{3i} + 1}{\sum_{i=1}^{q-1} z_{3i} + \theta} \right)^{|A|-1} \left(\frac{(\theta-1)z_{4j} + \sum_{i=1}^{q-1} z_{4i} + 1}{\sum_{i=1}^{q-1} z_{4i} + \theta} \right)^{k+1-|A|} \\ z'_{3j} = \lambda_j \left(\frac{(\theta-1)z_{2j} + \sum_{i=1}^{q-1} z_{2i} + 1}{\sum_{i=1}^{q-1} z_{2i} + \theta} \right)^{|A|-1} \left(\frac{(\theta-1)z_{1j} + \sum_{i=1}^{q-1} z_{1i} + 1}{\sum_{i=1}^{q-1} z_{1i} + \theta} \right)^{k+1-|A|} \\ z'_{4j} = \lambda_j \left(\frac{(\theta-1)z_{4j} + \sum_{i=1}^{q-1} z_{4i} + 1}{\sum_{i=1}^{q-1} z_{4i} + \theta} \right)^{k-|A|} \left(\frac{(\theta-1)z_{3j} + \sum_{i=1}^{q-1} z_{3i} + 1}{\sum_{i=1}^{q-1} z_{3i} + \theta} \right)^{|A|}, \end{cases} \quad (7.4)$$

here $j = 1, 2, 3, \dots, q-1$.

Denote

$$I_m = \{(z_1, \dots, z_{q-1}) \in \mathbb{R}^{q-1} : z_1 = \dots = z_m, z_{m+1} = \dots = z_{q-1} = 1\}, \quad (7.5)$$

$$M_m = \{(z^{(1)}, z^{(2)}, z^{(3)}, z^{(4)}) \in \mathbb{R}^{4(q-1)} : z^{(i)} \in I_m, i = 1, 2, 3, 4\}, \quad (7.6)$$

here $m = 1, 2, \dots, q-1$.

Lemma 7.1. *We have*

- 1) For any fixed $m \geq 1$, $\lambda > 0$ and

$$\lambda_i = \begin{cases} \lambda & \text{if } 1 \leq i \leq m \\ 1 & \text{if } m < i \leq q-1 \end{cases} \quad (7.7)$$

the set M_m is an invariant set with respect to the map K , i.e. $K(M_m) \subset M_m$.

- 2) For $\alpha = 0$ the sets M_m are invariant with respect to the map K for all $m = 1, 2, \dots, q-1$.

Case $\alpha \neq 0$. Let us consider the case $\alpha \neq 0$ and λ_i given by (7.7). For $\mathbf{z} \in M_m$ we denote $z_i = z_{ij}$, $i = 1, 2, 3, 4$; $j = 1, 2, \dots, m$. Then on the invariant set M_m the system of equations (7.3) has the following form

$$\begin{cases} z_1 = \lambda \left(\frac{(\theta+m-1)z_1 + q-m}{mz_1 + \theta + q-m-1} \right)^{k-|A|} \left(\frac{(\theta+m-1)z_2 + q-m}{mz_2 + \theta + q-m-1} \right)^{|A|} \\ z_2 = \lambda \left(\frac{(\theta+m-1)z_3 + q-m}{mz_3 + \theta + q-m-1} \right)^{|A|-1} \left(\frac{(\theta+m-1)z_4 + q-m}{mz_4 + \theta + q-m-1} \right)^{k+1-|A|} \\ z_3 = \lambda \left(\frac{(\theta+m-1)z_2 + q-m}{mz_2 + \theta + q-m-1} \right)^{|A|-1} \left(\frac{(\theta+m-1)z_1 + q-m}{mz_1 + \theta + q-m-1} \right)^{k+1-|A|} \\ z_4 = \lambda \left(\frac{(\theta+m-1)z_4 + q-m}{mz_4 + \theta + q-m-1} \right)^{k-|A|} \left(\frac{(\theta+m-1)z_3 + q-m}{mz_3 + \theta + q-m-1} \right)^{|A|}. \end{cases} \quad (7.8)$$

We introduce the notation

$$g_m(z) = \frac{(\theta + m - 1)z + q - m}{mz + \theta + q - m - 1}.$$

It is easy to prove the following

Lemma 7.2. *The function $g_m(z)$ is strictly decreasing for $0 < \theta < 1$, $1 \leq m \leq q - 1$ and strictly increasing for $1 < \theta$.*

Proposition 7.3. *Let $\mathbf{z} = (z_1, z_2, z_3, z_4)$ is a solution of the system of equations (7.8). If $z_i = z_j$ for some $i \neq j$, then $z_1 = z_2 = z_3 = z_4$.*

Consider now the anti-ferromagnetic Potts model (i.e. $0 < \theta < 1$).

Let $|A| = k$. Then system of equation (7.8) can be reduced to analyzing of the following system of equations

$$\begin{cases} z_2 = \lambda (g_m(z_3))^{k-1} \cdot g_m(\lambda (g_m(z_3))^k) \\ z_3 = \lambda (g_m(z_2))^{k-1} \cdot g_m(\lambda (g_m(z_2))^k). \end{cases} \quad (7.9)$$

Introducing the notation

$$\psi(z) = \lambda (g_m(z))^{k-1} \cdot g_m(\lambda (g_m(z))^k). \quad (7.10)$$

Then we reduce the system of equations (7.9) to the form

$$\begin{cases} z_2 = \psi(z_3) \\ z_3 = \psi(z_2). \end{cases} \quad (7.11)$$

The number of solutions of the system (7.11) coincides with the number of solutions of the equation $\psi(\psi(z)) = z$.

It is known (Theorem 3.1, see also [103, page 109]) that for anti-ferromagnetic case, there exists a unique translation-invariant Gibbs measure corresponding to the unique solution of the equation $z = \lambda g_m^k(z)$. We let z_* denote this solution.

Proposition 7.4. *For $k \geq 6$ and $\lambda \in (\lambda_{c_1}, \lambda_{c_2})$ the system of equations (7.11) has three solutions (z_*, z_*) , (z_2^*, z_3^*) , (z_3^*, z_2^*) , where $\lambda_{c_i} = b_i^k$, $i = 1, 2$ and*

$$\begin{aligned} b_1 &= \frac{(k-1 - \sqrt{k^2 - 6k + 1})(1-\theta)(\theta+q-1)z_*^{\frac{k-1}{k}}}{2(mz_* + \theta + q - m - 1)^2}, \\ b_2 &= \frac{(k-1 + \sqrt{k^2 - 6k + 1})(1-\theta)(\theta+q-1)z_*^{\frac{k-1}{k}}}{2(mz_* + \theta + q - m - 1)^2}. \end{aligned} \quad (7.12)$$

We have thus the following theorem.

Theorem 7.5. *Let $|A| = k$, $k \geq 6$ and $\lambda \in (\lambda_{c_1}, \lambda_{c_2})$. Then for the anti-ferromagnetic Potts model with the special external field (given by (7.7)) there are at least two H_A -weakly periodic (non-periodic) Gibbs measures, where $\lambda_{c_i} = b_i^k$, $i = 1, 2$.*

Case $\alpha = 0$. In this case the system of equations (7.3) on the invariant set M_m , $m = 1, 2, \dots, q - 1$ can be reduced to the following system of equations:

$$\begin{cases} z_1 = \left(\frac{(\theta+m-1)z_1+q-m}{mz_1+\theta+q-m-1} \right)^{k-|A|} \left(\frac{(\theta+m-1)z_2+q-m}{mz_2+\theta+q-m-1} \right)^{|A|} \\ z_2 = \left(\frac{(\theta+m-1)z_3+q-m}{mz_3+\theta+q-m-1} \right)^{|A|-1} \left(\frac{(\theta+m-1)z_4+q-m}{mz_4+\theta+q-m-1} \right)^{k+1-|A|} \\ z_3 = \left(\frac{(\theta+m-1)z_2+q-m}{mz_2+\theta+q-m-1} \right)^{|A|-1} \left(\frac{(\theta+m-1)z_1+q-m}{mz_1+\theta+q-m-1} \right)^{k+1-|A|} \\ z_4 = \left(\frac{(\theta+m-1)z_4+q-m}{mz_4+\theta+q-m-1} \right)^{k-|A|} \left(\frac{(\theta+m-1)z_3+q-m}{mz_3+\theta+q-m-1} \right)^{|A|} \end{cases} \quad (7.13)$$

The following proposition is similar to Proposition 7.3.

Proposition 7.6. *Let $m \in \{1, 2, \dots, q-1\}$ be fixed and $\mathbf{z} = (z_1, z_2, z_3, z_4)$ is a solution of the system of equations (7.13). If $z_i = z_j$ for some $i \neq j$, then $z_1 = z_2 = z_3 = z_4$.*

Theorem 7.7. *Let $|A| = k$ and $k \geq 6$. If one of the following conditions is satisfied*

- 1) $\frac{4k}{k+1+\sqrt{k^2-6k+1}} \leq q < \frac{4k}{k+1-\sqrt{k^2-6k+1}}$ and $0 < \theta < \theta_2$;
- 2) $q \leq \frac{4k}{k+1+\sqrt{k^2-6k+1}}$ and $\theta_1 < \theta < \theta_2$,

then there are at last $2^q - 2$ weakly periodic (non-periodic) Gibbs measures, where

$$\begin{aligned} \theta_1 &= \frac{4k - kq - q - q\sqrt{k^2 - 6k + 1}}{4k}, \\ \theta_2 &= \frac{4k - kq - q + q\sqrt{k^2 - 6k + 1}}{4k}. \end{aligned} \quad (7.14)$$

Remark 7.2. The new Gibbs measures described in Theorem 7.5 and Theorem 7.7 allow to describing a continuous set of non-periodic Gibbs measures (see Chapter 2 of [103] and [97] for such constructions) different from the previously known ones.

Remark 7.3. For the case $m = q - 1$ (see (7.6)), Theorem 7.7 coincides with Theorem 3 in [87].

References and comments. This review is based on works [10], [27], [28], [29], [34], [31], [32], [36], [39], [40], [45]-[48], [44], [50], [51], [63], [65], [69], [87]-[91], [96], [103]-[105], [107], [110]. Many of these papers written after 2013 and are related to the Potts model on trees.

In my opinion, one of nice results of the theory of Gibbs measures on trees is Theorem 3.3, which gives full description of TISGMs for q -state Potts model. Namely, it states that there are $\lfloor q/2 \rfloor$ distinct critical temperatures changing the number of TISGMs and there can be up to $2^q - 1$ such measures. Before of this result it was only known one critical temperature and q TISGMs [31],[32].

Applications of results of [65] allowed to give conditions of extremality of all TISGMs. Remaining results of this review are related to recently obtained results on boundary configurations, non-zero external fields, periodic and weakly periodic Gibbs measures and free energies of the Potts model.

For future reading see [3], [5], [8], [10], [11], [17], [19], [23], [24], [27], [35], [52],[60], [64], [72]-[77], [79], [80], [96]-[112], [122], [128], [130].

8. APPLICATIONS OF THE POTTS MODEL

The most studied model of statistical mechanics is the Ising model (i.e. 2-state Potts model), in MathSciNet there are about 6000 papers devoted to the problems related to Ising model. In [78] some physical motivations why the Ising model on

a Cayley tree is interesting are given. In particular, this model plays a very special role in statistical mechanics and gives the simplest nontrivial example of a system undergoing phase transitions.

The *Potts model* was introduced by R. B. Potts [84] as a lattice system with $q \geq 2$ spin states and nearest-neighbor interaction, to generalize of the Ising model.

The Potts model has been quickly picked up by a host of research in diverse areas. Here we give brief (not complete²) review of some interesting application of the Potts model:

8.1. Alloy behavior. An alloy is³ a combination of metals or metals combined with one or more other elements. Examples are combining the metallic elements gold and copper produces red gold, gold and silver becomes white gold, and silver combined with copper produces sterling silver.

By modeling of microstructural evolution one can study many metals processing companies because the alloys are usually designed computationally by tailoring their microstructural features (see [1] and references therein). These features entail grain size, particle/precipitate content, recrystallization fraction, and crystallographic texture, among others [83]. Moreover, in many industrial thermo-mechanical processes, various annealing phenomena (for example: recrystallization and grain growth) are incompletely understood. One of the computer simulation methods used to study such phenomena is the Monte Carlo Potts model (MCPM). This model has been used to simulate annealing phenomena such as grain growth in single- and two-phase polycrystalline materials, directional grain growth, particle pinning, static and dynamic recrystallization, microstructure, abnormal and nanocrystalline grain growth. The MCPM method has also demonstrated its applicability to modeling recrystallization in aluminum alloys.

To simulate recrystallization in a particle containing alloy, the paper [86] have coupled the finite element crystal plasticity method with MCPM.

In [1] a MCPM was used to model the primary recrystallization and grain growth in cold rolled single-phase Al alloy. The general vision of such modeling is to be able to optimize the microstructural features (grain size, recrystallization fraction, and crystallographic texture) during recrystallization and grain growth computationally in three dimensions in single-phase Al alloys. This simulation provides beneficial tools for understanding annealing and related phenomena in thermal treatments of rolled structures.

8.2. Cell sorting. In biology the cell (meaning “small room”) is the basic structural, functional, and biological unit of all known organisms. A cell is the smallest unit of life.

Cell migration is a central process in the development and maintenance of multicellular organisms. Tissue formation during embryonic development, wound healing and immune responses all require the orchestrated movement of cells in particular directions to specific locations. Cells often migrate in response to specific external signals, including chemical signals and mechanical signals [61].

²see <https://worldwidescience.org/topicpages/q/q-state+potts+model.html> for a list and abstracts of works related to Potts model.

³<https://en.wikipedia.org/wiki/Alloy>

Cellular Potts models (CPMs) (see [131] and references therein) are asynchronous probabilistic cellular automata developed specifically to model interacting cell populations. They are used to the field of cell and tissue biology. In particular, when the details of intercellular interaction are essentially determined by the shape and the size of the individual cells as well as the length of the contact area between neighboring cells.

A CPM is a discrete-time Markov chain, where the transition probabilities are specified with Gibbs measure corresponding to a Hamiltonian.

In [2] (see also the references therein) a CPM is considered, to simulate single cell migration over flat substrates with variable stiffness.

In the migration the cells sense their surroundings and respond to different types of signals. Cells preferentially crawl from soft to stiff substrates by reorganizing their cytoskeleton from an isotropic to an anisotropic distribution of actin filaments.

The following configurations are studied [2]:

1. a substrate including a soft and a stiff region,
2. a soft substrate including two parallel stiff stripes,
3. a substrate made of successive stripes with increasing stiffness to create a gradient and
4. a stiff substrate with four embedded soft squares.

For each case it is evaluated the morphology of the cell, the distance covered, the spreading area and the migration speed.

Cell sorting is the process of taking cells from an organism and separating them according to their type. The cells are labeled and tagged to identify areas of interest and their effect. They are separated based on differences in cell size, morphology (shape), and surface protein expression [95].

In the cell sorting while the surface-energy-driving mechanism is the same as for grain growth, biological cells have generally a fixed range of sizes. Thus the pattern cannot lose energy by coarsening, since cells cannot disappear, similar constrained evolution occurs in bubbles in magnetic films [134].

The differences in contact energies between cells of different types (differential adhesion) cause cell motion which reduces the pattern's energy. To take this into account the authors of [37] added an elastic-area constraint to the Hamiltonian of the Potts model: introduce a symbol τ for the cell type. In the model there are three cell types, "light" = l , "dark" = d and "medium" = M that is $\tau \in \{l, d, M\}$. The surface energy between two cells then depends on the types of the cells. Each cell still has a unique spin $\sigma \in \Phi$, and consists of all lattice sites with that spin, but there may be many cells of each type, i.e., with the same τ .

The extended Potts model is defined by the following

$$H(\sigma) = \sum_{\langle x,y \rangle} J(\tau(\sigma(x)), \tau(\sigma(y)))[1 - \delta_{\sigma(x)\sigma(y)}] \\ + \lambda \sum_{\text{spin types } \sigma} (a(\sigma) - A_{\tau(\sigma)})^2 \theta(A_{\tau(\sigma)}),$$

where $\tau(\sigma)$ is the type associated with the cell σ and $J(\tau, \tau')$ is the surface energy between types τ and τ' . λ is a Lagrange multiplier specifying the strength of the area constraint, $a(\sigma)$ the area of a cell σ , and A_{τ} , the target area for cells of type τ .

Because of the surface energy, each cell usually contains slightly fewer than A_τ , lattice sites. Moreover the biological aggregates are usually surrounded by a fluid medium (i.e. $\tau = M$), e.g., culture solution, substrate, or extracellular matrix, which is defined as a single cell with associated type, interaction energies, and unconstrained volume. Assume the target area A_M of the medium to be negative and to suppress the area constraint include

$$\theta(x) = \begin{cases} 0 & \text{if } x < 0 \\ 1 & \text{if } x > 0. \end{cases}$$

It is interesting to determine whether a model of this type exhibits biologically reasonable cell sorting. In coarsening, patterns are usually characterized by their side and area distributions and their moments, as well as the exponent describing the average rate of area growth. In cell sorting, the areas are approximately fixed so the area information is not useful.

In [37] the authors used Potts-model dynamics, with one Monte Carlo time step defined to be 16 times the number of spins in the array, but they suppress the nucleation of heterogeneous spins by requiring that a lattice site flip only to a spin belonging to one of its neighbors. It is found a long-distance cell movement leading to sorting with a logarithmic increase in the length scale of homogeneous clusters. Sorted clusters then round. Moreover two successive phases are found: a rapid boundary-driven creation of a low-cohesivity cell monolayer around the aggregate, and a slower boundary-independent internal rearrangement.

8.3. Financial engineering. In [92] based on a q -state Potts model a fast community detection algorithm is presented. Communities in networks (groups of densely interconnected nodes that are only loosely connected to the rest of the network) are found to coincide with the domains of equal spin value in the minima of a modified Potts spin glass Hamiltonian. Comparing global and local minima of the Hamiltonian allowed for the detection of overlapping (fuzzy) communities and quantifying the association of nodes to multiple communities as well as the robustness of a community.

In [127] a 3-state model based on the Potts model is proposed to simulate financial markets. The three states are assigned to "buy", "sell" and "inactive" states. The model shows the main stylized facts observed in the financial market: fat-tailed distributions of returns and long time correlations in the absolute returns.

The work [133] uses the Potts model to simulate and characterize the time evolution of a market time series. A two-dimensional 3-state Potts model is used to develop a stock price time series model.

This financial model imitates:

- (i) traders taking a selling position,
- (ii) traders taking a buying position, and
- (iii) traders taking no trading position,

which are classified as type 1, type 2, and type 3, respectively.

It is assumed (in [133]) that stock price behavior is strongly affected by the number of traders $\omega^{(1)}(t)$ (traders of type 1), $\omega^{(2)}(t)$ (traders of type 2), and $\omega^{(3)}(t)$ (traders of type 3).

Consider a single stock and assume that there are L^2 traders of this stock who are located in a square lattice: $L \times L \subset \mathbb{Z}^2$. Moreover, assume that each trader can trade a unit number of stock at each time $t \in \{1, 2, \dots, T\}$. At each time t , the fluctuation

of stock price process is strongly influenced by the number of traders who take buying positions and the number of traders who take selling positions. When the number of traders in selling positions is smaller than the number of traders in buying positions, the stock price is considered low by market participants, and the stock price gradually increases. The similar is true in the opposite case. In this proposed financial model, the clusters of parallel spins in the square-lattice Potts model are designated groups of market traders acting together.

In [137] permutation entropy and sample entropy are developed to the fractional cases, weighted fractional permutation entropy and fractional sample entropy. The effectiveness of these entropies as complexity measures is analyzed by application to the logistic map, which is a typical one-dimensional map creating chaos in some range of a parameter, such as the time series of some stock market indices and the price evolution of an artificial stock market using the Potts model. Moreover, the numerical research on nonlinear complexity behaviors is compared between the returns series of Potts financial model and the actual stock markets.

8.4. Flocking birds. Flocking⁴ is the behavior exhibited when a group of birds, called a flock, are foraging or in flight. There are parallels with the shoaling behavior of fish, the swarming behavior of insects, and herd behavior of land animals.

Examples: starlings are known for aggregating into huge flocks of hundreds to thousands of individuals, murmur at ions, which when they take flight altogether, render large displays of intriguing swirling patterns in the skies above observers.

Mathematical models used to study the flocking behaviors of birds can also generally be applied to the “flocking” behavior of other species.

In mathematical modeler, “flocking” is the collective motion by a group of self-propelled entities and is a collective animal behavior exhibited by many living beings. The flocking transition is an out-of-equilibrium phenomenon and abundant in nature (see [15] and references therein): from human crowds, mammalian herds, bird flocks, fish schools to unicellular organisms such as amoebae, bacteria, collective cell migration in dense tissues, and sub-cellular structures including cytoskeletal filaments and molecular motors.

The physics of flocking is also prevalent in nonliving substances such as rods on a horizontal surface agitated vertically, self propelled liquid droplets, liquid crystal hydrodynamics, and rolling colloids.

In basic models of flocking behavior the following three simple rules are taken into account:

- Separation - avoid crowding neighbors (short range repulsion)
- Alignment - steer towards average heading of neighbors
- Cohesion - steer towards average position of neighbors (long range attraction)

With these rules, the flock moves in an extremely realistic way, creating complex motion and interaction that would be extremely hard to create otherwise.

In [15] the 4-state active Potts model (APM) is considered, which has four internal states corresponding to four motion directions and is defined on a two-dimensional lattice with coordination number 4. Its two main ingredients leading to flocking are the local alignment interactions and self propulsion via biased hopping to neighboring sites without repulsive interactions.

⁴[https://en.wikipedia.org/wiki/Flocking_\(behavior\)](https://en.wikipedia.org/wiki/Flocking_(behavior))

A local alignment rule inspired by the ferromagnetic 4-state Potts model and self-propulsion via biased diffusion according to the internal particle states leads to flocking at high densities and low noise. The phase diagram of the APM is computed and the flocking dynamics in the region is explored, in which the high-density (liquid) phase coexists with the low-density (gas) phase and forms a fluctuating band of coherently moving particles. Moreover, as a function of the particle self-propulsion velocity, a novel reorientation transition of the phase-separated profiles from transversal to longitudinal band motion is revealed, which is absent in the active Ising model.

8.5. Flowing foams. Foams (see [18]) are complex fluids composed of gas bubbles tightly packed in a surfactant solution. In spite they generally consist only of Newtonian fluids, foam flow obeys nonlinear laws. This can result from non-affine deformations of the disordered bubble packing as well as from a coupling between the surface flow in the surfactant mono-layers and the bulk liquid flow in the films, channels, and nodes. A similar coupling governs the permeation of liquid through the bubble packing that is observed when foams drain due to gravity.

In [113] the CPM successfully simulates drainage and shear in foams. The CPM is used to investigate instabilities due to the flow of a single large bubble in a dry, mono-disperse two-dimensional flowing foam. It is shown that as in experiments in a Hele-Shaw cell⁵, above a threshold velocity the large bubble moves faster than the mean flow. These simulations reproduce analytical and experimental predictions for the velocity threshold and the relative velocity of the large bubble, demonstrating the utility of the CPM in foam rheology studies.

8.6. Image segmentation. In digital imaging, a pixel (or picture element) is a physical point in a raster⁶ image. The pixel is the smallest controllable element of a picture represented on the screen.

More pixels typically provide more accurate representations of the original image. In color imaging systems, a color is typically represented by three or four component intensities such as red, green, and blue, or cyan, magenta, yellow, and black (which can be assigned to states of the Potts model).

An image segmentation is⁷ the process of partitioning a digital image into multiple segments (sets of pixels, also known as image objects).

The segmentation is needed to simplify and/or change the representation of an image into something that is more meaningful and easier to analyze. This is the process of assigning a label to every pixel in an image such that pixels with the same label share certain characteristics.

In image analysis the problems involving incomplete data arise when some part of the data is missing or unobservable [16]. In this problems one wants to recover an original image which is hidden.

In [16] a Markov model-based image segmentation is studied, which involves hidden Markov random fields. The Potts model with external fields are used to better

⁵The term Hele-Shaw cell is commonly used for cases in which a fluid is injected into the shallow geometry from above or below the geometry, and when the fluid is bounded by another liquid or gas.

⁶a raster is a dot matrix data structure that represents a generally rectangular grid of colored points in a display medium.

⁷https://en.wikipedia.org/wiki/Image_segmentation

adequacy especially when the color proportions are very unbalanced in the images to be recovered.

As usual the pixels set S in image analysis is \mathbb{Z}^2 with the second order neighborhood system: for each site, the neighbors are the eight sites surrounding it.

The image segmentation involves observed and unobserved data to be recovered.

In [16] the unobserved data is modeled as a discrete Markov random field, where a commonly used distribution for the random field is the q -color Potts model with a non-zero external field. Moreover, an illustration of the advantages of introducing the external field is given with numerical experiments.

8.7. Medicine. Cancer is a group of diseases characterized by the uncontrolled growth of tumor⁸ cells that can occur anywhere in the body.

The paper [43] contains a survey of mathematical models that explicitly take into account the spatial architecture of three-dimensional tumours and address tumour development, progression and response to treatments. In particular, it discusses Potts models of epithelial acini, multicellular spheroids, normal and tumour spheroids and organoids, and multi-component tissues.

Here, following [9], [54], [125], [126], we give a review of the application of Potts model to cancer diseases.

In [9] the authors discussed CPM's application in developmental biology, focusing on the development of blood vessels, a process called vascular morphogenesis. A range of models focusing on uncovering the basic mechanisms of vascular morphogenesis are introduced: network formation and sprouting and then show how these models are extended with models of intracellular regulation and with interactions with the extracellular micro-environment. The integration of models of vascular morphogenesis in several examples of organ development in health and disease, including development, cancer, and age-related macular degeneration are reviewed. The computational efficiency of the CPM and the available strategies for the validation of CPM-based simulation models are presented.

Digital pathology imaging of tumor tissues, which captures histological details in high resolution, is fast becoming a routine clinical procedure.

In [54] (see also references therein) the authors considered the problem of modeling a pathology image with irregular locations of three different types of cells: lymphocyte, stromal, and tumor cells. A novel Bayesian hierarchical model is given, which incorporates a hidden Potts model to project the irregularly distributed cells to a square lattice and a Markov random field prior model (Gibbs measures of the Potts model) to identify regions in a heterogeneous pathology image. The model allowed to quantify the interactions between different types of cells, some of which are clinically meaningful.

The development of a tumor is initiated as the genomes of individual cells in an organism become destabilized, which usually kills cells, but in rare cases it modifies the properties of the cell in a way that allows it to proliferate and form a tumor. Despite a growing wealth of available molecular data, the growth of tumors, invasion of tumors into healthy tissue, and response of tumors to therapies are still poorly understood [126].

In [126] the authors review attempts to develop theoretical frameworks for collective cell behavior during tumor development. Mathematical descriptions of tumor growth

⁸Uncontrolled cells may form a mass called a tumor

and development range from continuum-level descriptions of gene-regulatory networks or tumor cell populations, to detailed, spatial models of individual and collective cell behavior. A cellular phenotype determines the success of a cancer cell in competition with its neighbors, irrespective of the genetic mutations or physiological alterations that gave rise to the altered phenotype. The CPM widely used to study the question what phenotypes can make a cell “successful” in an environment of healthy and cancerous cells. In particular, [126] reviews use of the CPM for modeling tumor growth, tumor invasion, and tumor progression.

In [125], to simulate the spatiotemporal evolution of the tumor, a mathematical model is constructed. Using both Potts model and nutrient competition a good visual simulation of tumor growth was provided, reproducing experimental results which also shows that the tumor growth is sensitive to the nutrient environment. It was noted that the results may have some medical signification:

(i) Tumors grow exponentially in the beginning. The tumor migrated toward the nutrient.

(ii) There are some differences in the dependence on nutrient between malignant cells and healthy cells. It may allow to control the nutrient environment in human host factitiously to avoid or cure cancer.

(iii) It may exist several critical nutrients which play a very different even opposite role in the growth process of malignant cells.

8.8. Neural network. A neural network is a network or circuit of neurons, or in a modern sense, an artificial neural network, composed of artificial neurons or nodes. Thus a neural network is either a biological neural network, made up of real biological neurons, or an artificial neural network, for solving artificial intelligence problems.

The q -state Potts-glass model is a symmetric feedback neural network with neurons of q states [56], [136]. Each neuron can be modeled with a Potts spin σ_i , where subscript i indicates neuron $i \in \{1, \dots, q\}$, that may represent the color or the shade of grey of a pixel in a pattern.

In [3] the critical properties of the Potts model with $q = 3$ and 8 states in one-dimension on directed small-world networks are investigated. The Potts model on these networks presents a second-order phase transition with a new set of critical exponents for $q = 3$. For $q = 8$ the system exhibits only a first-order phase transition.

The authors of [56] have studied the q -states Potts generalization of the Hopfield neural network evolving in parallel. Precise results are obtained on the asymptotic number of stored independent and identically distributed patterns so that either the patterns are fixed points of the dynamics or corrupted patterns get attracted to the original ones after one or several steps of the dynamics.

In [136] the authors have studied the q -state Potts-glass neural network with the pseudo-inverse rule. It is found that there exists a critical point of $q_c = 14$, below which the storage capacity and the retrieval quality can be greatly improved by introducing the pseudo-inverse rule. It was shown that the dynamics of the neural networks constructed with the two learning rules respectively are quite different; but however, regardless of the learning rules, in the q -state Potts-glass neural networks with $q \geq 3$ there is a common novel dynamical phase in which the spurious memories are completely suppressed. This property has never been noticed in the symmetric

feedback neural networks. Free from the spurious memories implies that the multi-state Potts-glass neural networks would not be trapped in the meta-stable states, which is a favorable property for their applications.

In very recent paper [128] using the techniques of neural networks, the three - dimensional, 5-state ferromagnetic Potts model on the cubic lattice and two-dimensional 3-state anti-ferromagnetic Potts model on the square lattice are studied. The whole or part of the theoretical ground state configurations of the studied models are considered as the training sets.

The results of the three-dimensional Potts model imply that the neural networks approach is as efficient as the traditional method since the signal of a first order phase transition, namely tunneling between two channels, determined by the neural networks method is as strong as that calculated with the Monte Carlo technique. Furthermore, the outcomes associated with the considered two-dimensional Potts model indicate even little partial information of the ground states can lead to conclusive results regarding the studied phase transition. These results demonstrate that the performance of neural networks, using the theoretical ground state configurations as the training sets, is impressive.

8.9. Phases transitions. In fact, the Potts model firstly appeared in statistical physics [4], [135]. In previous sections of this paper we gave strong mathematical presentation of this model for physical point of view.

It is known⁹ that as a model of a physical system, the Potts model is simple, but useful as a model system for the study of phase transitions. For example, the ferromagnetic Potts model on \mathbb{Z}^2 has a first order transition if $q > 4$. In case $q = 4$ a continuous transition is observed, as in the Ising model where $q = 2$. Other use of Potts model is found through the model's relation to percolation problems and the Tutte and chromatic polynomials found in combinatorics [114], [135].

For integer values of $q \geq 3$, the model displays the phenomenon of 'interfacial adsorption' with intriguing critical wetting properties when fixing opposite boundaries in two different states.

The q -state Potts model with $q \geq 3$ and an external field $\alpha \in \mathbb{R}$ on Cayley tree was considered in [81], [82]) using physical argumentation. In particular, they identified the critical temperature point T_c and also suggested an explicit critical boundary in the phase diagram for $\alpha \geq 0$.

It should be stressed that the phase transition occurring at these critical boundaries is not of type "uniqueness/non-uniqueness", with which we are concerned in the present book, but in fact the so-called "order/disorder" phase transition. The latter was studied rigorously in [35] in connection with the computational complexity of approximating the partition function of the Potts model. The useful classification of critical points deployed in [35] is based on the notion of *dominant phase*; in particular, a critical point is determined, from this point of view as a threshold beyond which only ordered phases are dominant.

8.10. Political trends. In [58] the Potts model is applied to Twitter data related to political trends. Twitter is a micro blogging environment where users post small messages, or Twitts, depicting their likes and dislike towards a certain topic, e.g. candidates to the next political elections.

⁹https://en.wikipedia.org/wiki/Potts_model

On the base of several electoral events and assuming a stationary regime, the authors of [58] found the following:

- (i) the maximization of the entropy singles out a microscopic model (single-Twitt-level) that coincides with a q -state Potts model having suitable couplings and external fields to be determined via an inverse problem from the two sets of data;
- (ii) correlations decay as $1/N_e$, where N_e is a small fraction of the mean number of Twitts;
- (iii) the simplest statistical models that reproduce these correlations are the multinomial distribution, characterized by q external fields, and the mean field Potts model, characterized by one coupling;
- (iv) this coupling turns out to be always close to its critical value.

8.11. Protein family. A protein is a polypeptide chain consists of a sequence of amino acids. The sequence of these amino acid units and one additional state for gaps or empty spaces. The gap state must be available for an amino acid to move when they fold into three dimensional structures to form domains.

A protein family¹⁰ is a group of evolutionary-related proteins. Usually a protein family has a corresponding gene family, in which each gene encodes a corresponding protein with a 1:1 relationship. The evolutionary history of a protein family is typically represented by a phylogenetic tree¹¹.

Proteins in a family descend from a common ancestor and typically have similar three-dimensional structures, functions, and significant sequence similarity. Two segments of a DNA may have shared ancestry because of three phenomena: either a speciation event, or a duplication event, or else a horizontal gene transfer event. Sequence homology is the biological homology between DNA, RNA, or protein sequences, defined in terms of shared ancestry in the evolutionary history of life.

Potts model is used to describe the sequence variability of sets of evolutionarily related protein sequences (i.e. homologous protein families). The notion of homologous protein families implies that present sequences derive from a common ancestor (see [94] and references therein).

In [94] the authors gave a principled way to correct for phylogenetic effects in the inference of Potts models from sequence data. Although the standard technique to account for these effects in co-evolutionary analysis relies on an empirical re-weighting of sequences. The method of [94] aims at doing so using the phylogenetic tree as well as an evolutionary model. The global nature of Potts models implies that the evolutionary model used should depend on the full sequence. An inference scheme is given that takes the phylogeny of a protein family into account in order to correct biases in estimating the frequencies of amino acids. Using artificial data, it is shown that a Potts model inferred using these corrected frequencies performs better in predicting contacts and fitness effect of mutations.

8.12. Protein folding. Protein folding is the physical process meaning that a protein chain acquires its native three-dimensional structure, a conformation that is usually biologically functional, in an expeditious and reproducible manner.

This subsection is based on [121].

¹⁰https://en.wikipedia.org/wiki/Protein_family

¹¹https://en.wikipedia.org/wiki/Phylogenetic_tree

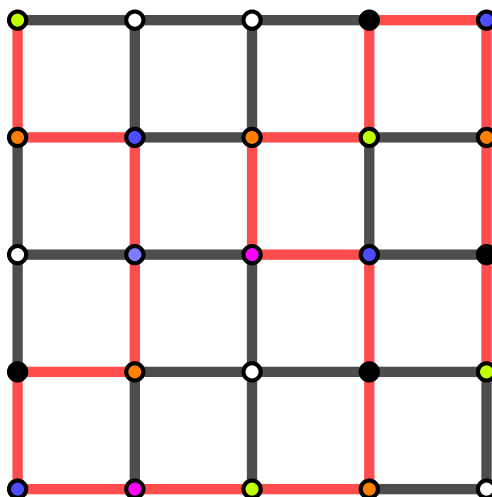


FIGURE 11. The two-dimensional protein is represented as a chain of amino acids (colored dots) connected by peptide bonds (red lines). The different colored dots occupied at lattice sites represent the different amino acids, the white dots represent the empty sites on the two dimensional lattice.

A Hamiltonian representing interacting amino acids on a lattice is given by

$$H(\sigma) = -\frac{1}{2} \sum_{i \neq j} J_{ij} \delta_{\sigma_i, \sigma_j} - \sum_i h_i \delta_{\sigma_i, \sigma_{q_0}},$$

where the external field h_i favors variables to align in σ_{q_0} ; that is forming domains of amino acid σ_{q_0} . Here J_{ij} is the pairwise interaction strength or the exchange parameter between variables σ_i and σ_j at two different lattice sites i and j . Note that the model allows each lattice site to have one out of q different states.

The Kronecker delta function and the negative sign in front of the first term of the Hamiltonian favor to have same amino acids at sites i and j . Due to this pairwise attractive interaction between same residues, domains of same amino acids is expected to be formed by folding the amino acid chain into a three dimensional structure. By the q -state Potts model, this structural formation is characterized by “ordering” of spin variables σ in a specific state.

In case when the entropy dominates at higher temperatures, the chain stretches inside the lattice (see Fig. 11) by moving amino acids to empty sites. When the energy dominates at lower temperatures, favored by the Potts model, same color amino acids cluster together by moving them closer. This clustering and stretching of same colors due to the competition between the energy and the entropy represents the protein folding and un-folding.

The general investigation of protein folding problem requires to solve the inverse Potts model, i.e. finding the coupling constants J_{ij} and h_i from the data base.

The main protein folding problem is understanding the question of how a protein’s amino acid sequence dictates its structure. The various interaction parameters inside the protein and the local environment are directly responsible for the folding. In [121] the authors studied the thermodynamic properties of the protein folding (the Potts model) using a statistical mechanics approach. Namely, converting the interacting

amino acids into an effectively non-interacting model using a mean-field theory, the Helmholtz free energy is found. Then by investigating the Helmholtz free energy, the properties of protein folding transition is qualitatively studied. It is shown that the protein folding phase transition is a strongly first order.

Potts models of protein sequence co-variation are statistical models constructed from the pair correlations observed in a multiple sequence alignment of a protein family. In ([53] see also references therein) the Potts models are reviewed to predict protein structure and sequence-dependent conformational free energy landscapes, to survey protein fitness landscapes and to explore the effects of epistasis on fitness.

8.13. Sociology. In [6], [115], [116] an application of Potts model to studies of human behavior is given: Nobel laureate Thomas Schelling published a seminal paper [115] which in addition to organized and economic explanations considers the possibility of micro-motive explanations for racial segregation. The premise is that individual decisions to avoid minority status (or to require being in a minority of some minimum size) could lead to the macro-effect of segregation. Schelling places vacancies, stars, and zeros randomly on a checkerboard and then iteratively considers the happiness of the stars and zeros with their local neighborhoods, moving an unhappy star or zero to the nearest vacant spot that meets their happiness criteria. Schelling works through many different experiments to come up with some very compelling results on segregation. From this model it seems that people do consciously or subconsciously segregate themselves from people who are different than they are.

The work [66] gives a similar premise to Schellings (that micro-motive explanations can lead to immigrant ghettos) with a more Potts-like model where the Hamiltonian measures the happiness of individuals with their neighbors, the temperature is viewed as a social temperature where warmer temperatures reflect facilitation of integration and assimilation, and at each step in the simulation two neighbors are able to exchange places with a probability based on the likelihood of the new state with respect to the current state. The paper [116] extends the work of [66] to address up to seven different ethnic groups.

Following [5] one can construct a Potts model for simulating human behavior in the following way. Use a lattice to depict your neighborhood, city, business, or any other venue in which people interact with one another. To have more groups, we can have elderly people, college roommates, families with teenagers, and families with small children. Assume that members of each of these groups of people are living together in a brand new development. Label the elderly with a 1, the college roommates with a 2, the families with teenagers with a 3, and the families with small children with a 4. The members of these groups have preferences about who they live near. For example, the elderly do not want to live next to the college roommates because of the large parties that they tend to throw. The couples with small children might want to live next to one another so that their kids can play together without going far from home. The Hamiltonian for this experiment would measure overall happiness as opposed to energy. Outside forces might be the price of other houses in other neighborhoods, proximity to work, or how much people like their current house. The Metropolis Algorithm could then be run to develop higher probabilities for lattice states with higher overall happiness. Eventually, we would likely see preferences playing out in the form of segregation. This is just a rough sketch of a Potts model scenario. This

may give an appreciation for the versatility of the Potts model when it comes to real world situations.

8.14. Spin glasses. A glassy system is complex system that exhibits a very slow dynamics that prevents it from reaching the equilibrium state. Examples are real glasses, spin glasses, supercooled liquids, polymers, granular material, colloids, ionic conductors, orientational glasses, and vortex glasses [26].

A spin glass is a model¹² of a certain type of magnet. Magnetic spins are the orientation of the north and south magnetic poles in three-dimensional space. In ferromagnetic solids, component atoms magnetic spins all align in the same direction. Spin glasses are contrasted with ferromagnetism as “disordered” magnets in which their atoms spins are not aligned in a regular pattern.

The complex internal structures that arise within spin glasses are termed “metastable” because they are “stuck” in stable configurations other than the lowest-energy configuration. The mathematical complexity of these structures is difficult but fruitful to study experimentally or in simulations; with applications to physics, chemistry, materials science and artificial neural networks in computer science.

The Potts model of spin glass is defined by the Hamiltonian [26]:

$$H(\sigma, s) = -qJ \sum_{\langle i,j \rangle} [\delta_{\sigma_i \sigma_j} (\epsilon_{ij} s_i s_j + 1) - 2],$$

where associated with each lattice site is an Ising spin $s_i \in \{-1, 1\}$ and a q -state Potts spin $\sigma_i \in \{1, \dots, q\}$. The sum is extended over all nearest-neighbor sites, $\epsilon_{i,j} = \pm 1$ is a random quenched variable, and J is the strength of interaction.

The model is a superposition of a ferromagnetic q -state Potts model and a $\pm J$ Ising spin glass model [62].

In [26] it is shown that this model exhibits for all q a spin glass transition at $T_{SG}(q)$ and a percolation transition at higher temperature $T_P(q)$. It is shown that for all values of $q > 1$ at $T_P(q)$ there is a thermodynamic transition in the universality class of a ferromagnetic q -state Potts model. Moreover, the efficiency of the cluster dynamics is compared with that of standard spin-flip dynamics.

There are variations of the Potts spin glass model, which has been studied extensively in the physics literature (see, e.g., [13], [62], [79] and references therein).

8.15. Storage capacity. Storage capacity measures how much data a computer system may contain. For an example, a computer with a 500GB hard drive has a storage capacity of 500 gigabytes.

A Potts unit (spin value) can be regarded (see [57]) in the neuroscience context as representing a local subnetwork or cortical patch of real neurons, endowed with its set of dynamical attractors, which span different directions in activity space, and are therefore converted to the states of the Potts unit (which is defined precisely as having states pointing each along a different dimension of a simplex). One can define the model as an auto-associative network of Potts units interacting through tensor connections. The memories are stored in the weight matrix of the network and they are fixed: each memory μ is a vector or list of the states taken in the overall activity configuration by each unit.

Take each Potts unit to have S possible active states, labeled e.g. by the index k , as well as one quiescent state, $k = 0$, when the unit does not participate in the

¹²https://en.wikipedia.org/wiki/Spin_glass

activity configuration of the memory. Using this model in [57] the storage capacity of the Potts network is studied. The storage capacity calculation, performed using replica tools, is limited to fully connected networks, for which a Hamiltonian can be defined. To extend the results to the case of intermediate partial connectivity, the self-consistent signal-to-noise analysis is derived for the Potts network; and the implications for semantic memory in humans is discussed.

In [42] the theory of neural networks is extended to include discrete neurons with q , $q \geq 2$ discrete states. The dynamics of such systems are studied by using Potts model. The maximum number of storage patterns is found to be proportional to $Nq(q-1)$, where q is the number of Potts states and N is the size of the network.

It is known (see [49]) that the capacity to store information in any device, and in particular the capacity to store concepts in the human brain, is limited. In [49] it is shown in a minimal model of semantic memory, and in progressive steps, how one can expect the storage capacity to behave depending on the parameters of the system. It was deduced the minimum requirements of any model of this kind in order to have a high capacity. The calculation specifies that in the Potts model the number of concepts that can be stored is neither linear nor an arbitrary power of the number S of values a feature can take, but quadratic in S .

8.16. Symmetric channels. Symmetric channels on q symbols have the state space $\{1, \dots, q\}$ and $q \times q$ -matrices:

$$\mathbf{M} = \begin{pmatrix} 1 - (q-1)\delta & \delta & \delta & \dots & \delta \\ \delta & 1 - (q-1)\delta & \delta & \dots & \delta \\ \dots & \vdots & \dots & \vdots & \dots \\ \delta & \delta & \delta & \dots & 1 - (q-1)\delta \end{pmatrix}, \quad (8.1)$$

with $\lambda_2(M) = 1 - q\delta$.

Depending on the sign of $\lambda_2(M)$ we distinguish between ferromagnetic Potts models where $\lambda_2(M) > 0$, and anti-ferromagnetic models where $\lambda_2(M) < 0$. In case $1 - (q-1)\delta = 0$ we obtain the model of proper colorings of the tree:

$$\mathbf{M} = \begin{pmatrix} 0 & (q-1)^{-1} & (q-1)^{-1} & \dots & (q-1)^{-1} \\ (q-1)^{-1} & 0 & (q-1)^{-1} & \dots & (q-1)^{-1} \\ \dots & \vdots & \dots & \vdots & \dots \\ (q-1)^{-1} & (q-1)^{-1} & (q-1)^{-1} & \dots & 0 \end{pmatrix}. \quad (8.2)$$

Several bounds for the reconstruction problem (for q -state Potts models on a Cayley tree of order $k \geq 2$) are known (see [67]-[69], [122]):

- If $k\lambda_2^2(M) > 1$ then the reconstruction problem is solvable.
- If $k|\lambda_2(M)| \leq 1$, then the reconstruction problem is unsolvable.
- If $k\lambda_2(M) > 1$ and q is sufficiently large, then the reconstruction problem is solvable.
- If $k\frac{(1-q\delta)^2}{1-(q-2)\delta} \leq 1$ then the reconstruction problem is unsolvable.

As it was mentioned above the most general result on reconstruction is the Kesten-Stigum bound [44] which says that reconstruction holds when $k\lambda_2^2 > 1$.

In [122] the author proved the first exact reconstruction threshold in a non-binary model establishing the Kesten-Stigum bound for the 3-state Potts model on regular trees of large degree. The Kesten-Stigum bound is not tight for the q -state Potts model when $q \geq 5$. Moreover, asymptotics for these reconstruction thresholds are determined.

It was studied in genetics (see e.g. [14], [124]) an information flow can be used to represent propagation of a genetic property from ancestor to its descendants. In communication theory, this process represents a communication network on the tree where information is transmitted from the root of the tree. Moreover, the process was studied in statistical physics, see e.g. [7], [40]. More precisely, in statistical physics a non-uniqueness of the Gibbs measure means that for all n there exists σ_n such that the distribution of σ_ρ given σ_n has total variation distance at least $\delta > 0$ from uniform. This is a weaker condition than reconstruction solvability and it was studied in statistical physics for Ising and Potts models (see [36], [38], [85]).

The crucial role of the reconstruction problem in Phylogeny was demonstrated in [70] and [71].

8.17. Technological processes. Technology means activities, because it is in constant development. In general technological processes can be design processes, making processes and processes in the phase of using and assessing technology [132].

Ostwald ripening¹³ is a phenomenon observed in solid solutions or liquid sols that describes the change of an inhomogeneous structure over time, i.e., small crystals or sol particles dissolve, and redeposit onto larger crystals or sol particles. The Ostwald ripening is generally found in water-in-oil emulsions, while flocculation is found in oil-in-water emulsions.

Some analytic methods used to model processes such as grain growth and Ostwald ripening by many simplifying assumptions.

In [123] the q -state Potts model was adapted to study grain growth (development). By this model it was treated the next level of complexity by incorporating grain boundary topology. Moreover, the growth kinetics of a two dimensional, connected assembly of mutually interacting grains are described.

Now following [129] we give one more application of the Potts model [129]. Markets often demand small quantities of many different components with highly specialized performance requirements. Therefore, the development cost of each component cannot be amortized over large numbers and becomes prohibitive. Good predictive tools are necessary for reduction of the development cost. It has been proved that the Potts model is a powerful and useful tool for simulating a wide variety of microstructural evolution problems both during processing and during component use. In [129] the use and application of the Potts model to Ostwald ripening is presented.

Here, to see how the Potts model appears, we give phase equilibria characteristics of [129]:

Consider \mathbb{Z}^2 as the lattice of the q -state Potts model. A canonical ensemble of sites, which may be visualized as building blocks of the microstructure, populates a simulation lattice. These sites possess certain energies based on their inherent characteristics and on their interactions with their neighboring domains and evolve to minimize the total free energy of the system.

¹³https://en.wikipedia.org/wiki/Ostwald_ripening

The evolution mechanism is that each domain can be modified based on the energetics of the modification being considered. Then a digitized microstructures can be represented on \mathbb{Z}^2 with a periodic boundary conditions. The components necessary for Ostwald ripening can be incorporated into the Potts model by populating the simulation lattice with a canonical ensemble having two components designated as A and B . The A -sites are the primary building blocks of the grains and the B -sites of the matrix, as shown in Fig. 12.

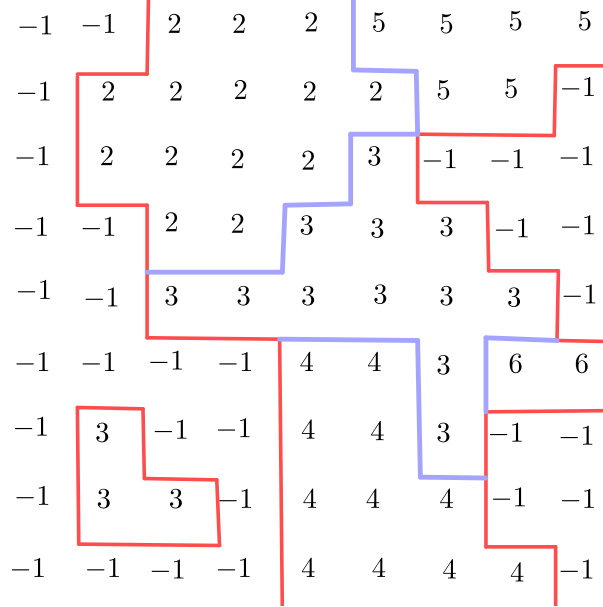


FIGURE 12. Illustration of the technique used to digitize microstructures. The grains in a liquid with grain boundaries (blue) and solid-liquid interfaces (red) are shown. The B -sites are all the sites labeled “-1” and A -sites are labeled with positive integers.

The two components, A and B , must separate into two phases, grains dispersed in a matrix. The two phases were generated by defining bond energies between the A - and B -sites, so that the components would segregate into two phases. The $A - B$ bonds are assigned higher energies than $A - A$ or $B - B$ bonds. Thus the system minimizes its energy by segregating the A - and B -sites into two phases.

8.18. Wetting transition. Here we follow [55] (see also references therein). The study of liquid behavior on a surface is a topic that is receiving increasing interest due to its diverse applications.

Examples of application are: microfluidics for biotechnology, textile lubrication, and self-cleaning. The inspiration arose in nature, more precisely from the plant (the lotus), whose leaves have a natural hydrophobicity.

Based on the surface structure of the leaf, similar artificial rough surfaces were produced. A drop of water on this type of surface can exhibit two states of wettability:

- Wenzel state, in which the drop of water penetrates the surface cavities;
- Cassie-Baxter (CB) state, in which the drop remains on the top of the pillars, as in the lotus leaf.

The Wenzel approach considers that the liquid fills up completely the grooves on the rough surface increasing thus the total area of the liquid-solid interface.

The CB approach assumes that air pockets are trapped inside the grooves, and thus, that the liquid only contacts the solid at the top of the asperities. Thus, the drop sits on a composite surface comprised of solid and trapped air.

The energy barrier between the CB-Wenzel state transition is given as a product of the following factors: the pillar height, pillar thickness, and the area that the droplet occupies between the pillars. This energy barrier separating the states may be large enough to prevent a spontaneous transition from occurring.

The work [55] is based on a two-dimensional Potts model of a droplet placed on a regularly patterned surface of pillars of different heights and interspacing.

The model is defined as follows. Consider a square lattice, where to each network site, i , a value $\sigma_i \in \Phi = \{1, \dots, q\}$ is given. The set Φ is labels associated with the different media: air, liquid, solid etc.

The Hamiltonian (the total energy) of the system is

$$H(\sigma) = \frac{1}{2} \sum_{\langle i,j \rangle} \gamma_{\sigma_i \sigma_j} (1 - \delta_{\sigma_i \sigma_j}) + \lambda (A_{\sigma=1} - A_T)^2 + mg \sum_i \delta_{1\sigma_i} h_i,$$

where $\sigma = \{\sigma_i : i \in \mathbb{Z}^2\}$ the configuration (the labels on the sites of the lattice) and $\gamma_{\sigma_i \sigma_j}$ is the interfacial energy between neighboring sites belonging to different media [37]. The second term corresponds to an elastic compression energy: $A_{\sigma=1}$ is the drop area, A_T is a target area, and λ is a Lagrange multiplier related to the inverse of the liquid compressibility [41]. This term is required to avoid the droplet disappearance by energy minimization. The last term is the contribution from the gravitational energy, where g is the acceleration of gravity¹⁴ and h_i is the vertical coordinate of a label belonging to the droplet defined as having unit mass ($m_{\sigma=1} = 1$).

In [117] (see also the references therein) the transition and the influence of the energy barrier on the transition through thermodynamics and molecular dynamics models.

In [55] Potts model simulation compared with the studies developed [117], [118] employing thermodynamics and two-dimensional molecular dynamics.

ACKNOWLEDGEMENTS

I thank my coauthors who collaborated with me to develop the theory of Gibbs measures: L.V.Bogachev, G.I.Botirov, M.Cassandro, D.Gandolfo, N.N.Ganikhodjaev, F.Haydarov, F.Henning, O.Khakimov, R.Khakimov, S.Kissel, C.Külske, A.LeNy, L.Liao, I.Merola, F.M.Mukhamedov, M.Rahmatullaev, J.Ruiz, Yu.M.Suhov, J.P.Tian, Y.Velenik and many others.

REFERENCES

- [1] K. Adam, D. Zöllner, D.P. Field, *3D microstructural evolution of primary recrystallization and grain growth in cold rolled single-phase aluminum alloys*, Modelling Simul. Mater. Sci. Eng. **26** (2018), 035011 (16 pages).
- [2] R. Allena, M. Scianna, L. Preziosi, *A cellular Potts model of single cell migration in presence of durotaxis*. Math. Biosci. **275** (2016), 57–70.
- [3] É.O. Aquino, F.W. Lima, A.D. Araújo, F.R.N. Costa, *Potts model in one-dimension on directed small-world networks*. J. Stat. Phys. **171**(6) (2018), 1112–1121.
- [4] R.J. Baxter, *Exactly solved models in statistical mechanics*, Reprint of the 1982 original. Academic Press, Inc. [Harcourt Brace Jovanovich, Publishers], London, (1989).

¹⁴The gravity can be neglected in case of very small droplets.

- [5] L. Beaudin, *A Review of the Potts Model*, Rose-Hulman Undergraduate Math. Jour. **8**(1) (2007), Article 13, (25 pages).
- [6] L. Beaudin, J. Ellis-Monaghan, G. Pangborn, R. Shrock, *A little statistical mechanics for the graph theorist*. Discrete Math. **310**(13-14) (2010), 2037–2053.
- [7] P.M. Bleher, J. Ruiz, V.A. Zagrebnov, *On the purity of the limiting Gibbs state for the Ising model on the Bethe lattice*. J. Stat. Phys. **79** (1995), 473–482.
- [8] P. Bleher, M. Lyubich, R. Roeder, *Lee-Yang-Fisher zeros for the DHL and 2D rational dynamics, II. Global pluripotential interpretation*. J. Geom. Anal. **30**(1) (2020), 777–833.
- [9] S.E.M. Boas, Y. Jiang, R.M.H. Merks, S.A. Prokopiou, E.G. Rens, *Cellular Potts model: applications to vasculogenesis and angiogenesis*. Probabilistic cellular automata, 279–310, Emerg. Complex. Comput., 27, Springer, Cham, 2018.
- [10] L.V. Bogachev, U.A. Rozikov, *On the uniqueness of Gibbs measure in the Potts model on a Cayley tree with external field*. J. Stat. Mech. Theory Exp. **7** (2019), 073205, 76 pp.
- [11] G.I. Botirov, U.A. Rozikov, *The Potts model with competing interactions on the Cayley tree: the contour method*. Theoret. Math. Phys. **153**(1) (2007), 1423–1433.
- [12] T. Brookings, J.M. Carlson, J. Doyle, *Three mechanisms for power laws on the Cayley tree*. Phys. Rev. E. **72** (2005), 056120, 18 pp.
- [13] F. Caltagirone, G. Parisi, T. Rizzo, *Dynamical critical exponents for the mean-field Potts glass*. Phys. Rev. E, **85** (2012), 051504.
- [14] J. Cavender, *Taxonomy with confidence*, Math. BioSci. **40** (1978), 271–280.
- [15] S. Chatterjee, M. Mangeat, R. Paul, H. Rieger, *Flocking and reorientation transition in the 4-state active Potts model*, EPL (Europhysics Letters), **130**(6) (2020), 66001, (8 pages).
- [16] G. Celeux, F. Forbes, N. Peyrard. *EM-based image segmentation using Potts models with external field*. [Research Report] RR-4456, INRIA. 2002. inria-00072132.
- [17] L. Cioletti, R. Vila, *Graphical representations for Ising and Potts models in general external fields*. J. Stat. Phys. **162**(1) (2016), 81–122.
- [18] S. Cohen-Addad, R. Höhler, O. Pitois, *Flow in foams and flowing foams*, Annual Review of Fluid Mechanics, **45** (2013), 241–267.
- [19] L. Coquille, H. Duminil-Copin, D. Ioffe, Y. Velenik, *On the Gibbs states of the noncritical Potts model on \mathbb{Z}^2* . Probab. Theory Related Fields **158**(1-2) (2014), 477–512.
- [20] L. Coquille, *Examples of DLR states which are not weak limits of finite volume Gibbs measures with deterministic boundary conditions*, Jour. Stat. Phys. **159**(4) (2015), 958–971.
- [21] C. Daskalakis, E. Mossel, S. Roch, *Evolutionary trees and the Ising model on the Bethe lattice: a proof of Steel’s conjecture*. Probab. Theory Related Fields. **149**(1-2) (2011), 149–189.
- [22] A. Dembo, A. Montanari, A. Sly, N. Sun, *The replica symmetric solution for Potts models on d -regular graphs*. Comm. Math. Phys. **327** (2014), 551–575.
- [23] H. Duminil-Copin, V. Sidoravicius, V. Tassion, *Continuity of the phase transition for planar random-cluster and Potts models with $1 \leq q \leq 4$* . Comm. Math. Phys. **349**(1) (2017), 47–107.
- [24] O.N. Feldheim, Y. Spinka, *Long-range order in the 3-state antiferromagnetic Potts model in high dimensions*. J. Eur. Math. Soc. (JEMS) **21**(5) (2019), 1509–1570.
- [25] M. Formentin, C. Külske, *A symmetric entropy bound on the non-reconstruction regime of Markov chains on Galton-Watson trees*. Electron. Commun. Probab. **14** (2009), 587–596.
- [26] G. Franzese, A. Coniglio, *Phase transitions in the Potts spin-glass model*, Phys. Rev. E, **58**(3) (1998), 2753–2759.
- [27] S. Friedli, Y. Velenik, *Statistical mechanics of lattice systems. A concrete mathematical introduction*. Cambridge University Press, Cambridge, 2018.
- [28] D. Gandolfo, M.M. Rakhmatullaev, U.A. Rozikov, J. Ruiz, *On free energies of the Ising model on the Cayley tree*. Jour. Stat. Phys. **150**(6) (2013), 1201–1217.
- [29] D. Gandolfo, M.M. Rakhmatullaev, U.A. Rozikov, *Boundary conditions for translation-invariant Gibbs measures of the Potts model on Cayley trees*. J. Stat. Phys. **167**(5) (2017), 1164–1179.
- [30] N.N. Ganikhodjaev, *The Potts model on \mathbb{Z}^d with countable set of spin values*. J. Math. Phys. **45**(3) (2004), 1121–1127.
- [31] N.N. Ganikhodjaev, *On pure phases of the three-state ferromagnetic Potts model on the second-order Bethe lattice*. Theor. Math. Phys. **85**(2) (1990), 1125–1134.

- [32] N.N. Ganikhodzhaev, *On pure phases of the ferromagnetic Potts model Bethe lattices*, Dokl. AN Uzbekistan. No. 6-7 (1992), 4–7.
- [33] N.N. Ganikhodzhaev, U.A. Rozikov, *The Potts model with countable set of spin values on a Cayley tree*, Lett. Math. Phys. **75**(2) (2006), 99–109.
- [34] N.N. Ganikhodzhaev, U.A. Rozikov, *Description of periodic extreme Gibbs measures of some lattice models on a Cayley tree*. Theoret. Math. Phys. **111**(1) (1997), 480–486.
- [35] A. Galanis, D. Štefankovič, E. Vigoda, L. Yang, *Ferromagnetic Potts model: refined #BIS-hardness and related results*. SIAM J. Comput. **45**(6) (2016), 2004–2065.
- [36] H.O. Georgii, *Gibbs Measures and Phase Transitions*, Second edition. de Gruyter Studies in Mathematics, 9. Walter de Gruyter, Berlin, 2011.
- [37] F. Graner, J. Glazier, *Simulation of biological cell sorting using a two-dimensional extended Potts model*. Phys. Rev. Lett. **69**(13) (1992), 2013–2017.
- [38] W.M. Haddad, *A dynamical systems theory of thermodynamics*. Princeton Series in Applied Mathematics. Princeton University Press, Princeton, NJ, 2019.
- [39] O. Häggström, C. Külske, *Gibbs properties of the fuzzy Potts model on trees and in mean field*, Markov Proc. Rel. Fields **10**(3) (2004), 477–506.
- [40] Y. Higuchi, *Remarks on the limiting Gibbs states on a $(d + 1)$ -tree*. Publ. RIMS, Kyoto Univ. **3** (1977), 335–348.
- [41] M.A. Idiart, Y. Levin, *Rupture of a liposomal vesicle*. Phys. Rev. E. **69**(6) (2004), 061922.
- [42] I. Kanter, *Potts-glass models of neural networks*. Phys. Rev. A (3) **37**(7) (1988), 2739–2742.
- [43] A.Karolak, D.A.Markov, L.J. McCawley, K.A.Rejniak, *Towards personalized computational oncology: from spatial models of tumour spheroids, to organoids, to tissues*. J. R. Soc. Interface, **15** (2018), 20170703, (16 pages).
- [44] H. Kesten, B.P. Stigum, *Additional limit theorem for indecomposable multi-dimensional Galton-Watson processes*, Ann. Math. Statist. **37** (1966), 1463–1481.
- [45] R.M. Khakimov, *On the existence of periodic Gibbs measures for the Potts model on a Cayley tree*. (Russian) Uzbek. Mat. Zh. **3** (2014), 134–142.
- [46] R.M. Khakimov, *New Periodic Gibbs Measures for q -state Potts Model on a Cayley Tree*. Jour. Siberian Federal Univ. Math. and Phys. **7**(3) (2014), 297–304.
- [47] R.M. Khakimov, M.T. Makhammadaliev, *Translation invariance of periodic Gibbs measures for the Potts model on the Cayley tree*. Theoret. Math. Phys. **199**(2) (2019), 726–735.
- [48] R.M. Khakimov, F.Kh. Khaidarov, *Translation-invariant and periodic Gibbs measures for the Potts model on a Cayley tree*. Theoret. Math. Phys. **189**(2) (2016), 1651–1659.
- [49] E. Kropff, A. Treves, *The storage capacity of Potts models for semantic memory retrieval*. J. Stat. Mech. Theory Exp. **8** (2005), P08010, 19 pp.
- [50] C. Külske, U.A. Rozikov, R.M. Khakimov, *Description of the translation-invariant splitting Gibbs measures for the Potts model on a Cayley tree*. J. Stat. Phys. **156**(1) (2014), 189–200.
- [51] C. Külske, U.A. Rozikov, *Fuzzy transformations and extremality of Gibbs measures for the Potts model on a Cayley tree*. Random Structures Algorithms. **50**(4) (2017), 636–678.
- [52] C. Külske, D. Meißner, *Stable and metastable phases for the Curie-Weiss-Potts model in vector-valued fields via singularity theory*. J. Stat. Phys. **181**(3) (2020), 968–989.
- [53] R. M. Levy, A. Haldane, W. F. Flynn, *Potts Hamiltonian models of protein co-variation, free energy landscapes, and evolutionary fitness*, Curr. Opin. Struct. Biol. **43** (2017), 55–62.
- [54] Q. Li, X. Wang, F. Liang, F. Yi, Y. Xie, A. Gazdar, G. Xiao, *A Bayesian hidden Potts mixture model for analyzing lung cancer pathology images*, Biostatistics, **20**(4) (2019), 565–581.
- [55] D.M. Lopes, J.C. M. Mombach, *Two-dimensional wetting transition modeling with the Potts model*, Braz. J. Phys. **47** (2017), 672–677.
- [56] M. Löwe, F. Vermet, *The capacity of q -state Potts neural networks with parallel retrieval dynamics*. Statist. Probab. Lett. **77**(14) (2007), 1505–1514.
- [57] M. Naim, V. Boboeva, C.J. Kang, A. Treves, *Reducing a cortical network to a Potts model yields storage capacity estimates*. J. Stat. Mech. Theory Exp. **4** 2018, 043304, 35 pp.
- [58] L. Nicolao, M. Ostilli, *Critical states in political trends. How much reliable is a poll on Twitter?* Phys. A **533** (2019), 121920, 18 pp.
- [59] E.P. Normatov, U.A. Rozikov, *A description of harmonic functions using the properties of the group representation of the Cayley tree*. Math. Notes. **79**(3-4) (2006), 399–407.

- [60] M. Ostilli, F. Mukhamedov, *1D three-state mean-field Potts model with first- and second-order phase transitions*. Phys. A **555** (2020), 124415, 10 pp.
- [61] M. Mak, F. Spill, K. Roger, M. Zaman, *Single-cell migration in complex microenvironments: mechanics and signaling dynamics*. Journal of Biomechanical Engineering. **138**(2) (2016), 021004 (8 pages).
- [62] E. Marinari, S. Mossa, G. Parisi, *Glassy Potts model: A disordered Potts model without a ferromagnetic phase*. Phys. Rev. B, **59** (1999), 8401.
- [63] J.B. Martin, *Reconstruction thresholds on regular trees*. Discrete random walks (Paris, 2003), 191–204 (electronic), Discrete Math. Theor. Comput. Sci. Proc., AC, Assoc. Discrete Math. Theor. Comput. Sci., Nancy, 2003.
- [64] P.P. Martin, S.F. Zakaria, *Zeros of the 3-state Potts model partition function for the square lattice revisited*. J. Stat. Mech. Theory Exp. **8** (2019), 084003, 25 pp.
- [65] F. Martinelli, A. Sinclair, D. Weitz, *Fast mixing for independent sets, coloring and other models on trees*. Random Structures and Algorithms, **31** (2007), 134–172.
- [66] H. Meyer-Ortmanns, *Immigration, integration and ghetto formation*, Internat. J. Modern Phys. C **14**(3) (2003), 311–320.
- [67] E. Mossel, *Reconstruction on trees: beating the second eigenvalue*, Ann. Appl. Probab. **11**(1) (2001), 285–300.
- [68] E. Mossel, Y. Peres, *Information flow on trees*, Ann. Appl. Probab. **13**(3) (2003), 817–844.
- [69] E. Mossel, *Survey: Information flow on trees*. Graphs, morphisms and statistical physics, 155–170, DIMACS Ser. Discrete Math. Theoret. Comput. Sci., 63, Amer. Math. Soc., Providence, RI, 2004.
- [70] E. Mossel, *On the impossibility of reconstructing ancestral data and phylogenies*, J. Comput. Biol. **10**(5) (2003), 669–678.
- [71] E. Mossel, M. Steel, *A phase transition for a random cluster model on phylogenetic trees*, Math. Biosci. **187**(2) (2004), 189–203.
- [72] F.M. Mukhamedov, U.A. Rozikov, J.F. Mendes, *On contour arguments for the three state Potts model with competing interactions on a semi-infinite Cayley tree*. J. Math. Phys. **48**(1) (2007), 013301, 14 pp.
- [73] F.M. Mukhamedov, U.A. Rozikov, *On Gibbs measures of p -adic Potts model on the Cayley tree*, Indag. Math., New Ser. **15** (2004), 85–100.
- [74] F.M. Mukhamedov, U.A. Rozikov, *On inhomogeneous p -adic Potts model on a Cayley tree*, Infin. Dimens. Anal. Quantum Probab. Relat. Top. **8** (2005), 277–290.
- [75] F.M. Mukhamedov, U.A. Rozikov, J.F.F. Mendes, *On phase transitions for p -adic Potts model with competing interactions on a Cayley tree*, in p -Adic Mathematical Physics: Proc. 2nd Int. Conf., Belgrade, 2005 (Am. Inst. Phys., Melville, NY, 2006), AIP Conf. Proc. 826, pp. 140–150.
- [76] F.M. Mukhamedov, O.N. Khakimov, *On periodic Gibbs measures of p -adic Potts model on a Cayley tree*. p -Adic Numbers Ultrametric Anal. Appl. **8**(3) (2016), 225–235.
- [77] F.M. Mukhamedov, O.N. Khakimov, *Phase transition and chaos: P -adic Potts model on a Cayley tree*. Chaos Solitons Fractals, **87** (2016), 190–196.
- [78] E. Müller-Hartmann, *Theory of the Ising model on a Cayley tree*, Z. Phys. B **27** (1977), 161–168.
- [79] D. Panchenko, *Free energy in the Potts spin glass*. Ann. Probab. **46**(2) (2018), 829–864.
- [80] U. Paun, *G method in action: normalization constant, important probabilities, and fast exact sampling for Potts model on trees*. Rev. Roumaine Math. Pures Appl. **65**(2) (2020), 101–128.
- [81] F. Peruggi, F. di Liberto, G. Monroy, *The Potts model on Bethe lattices. I. General results*. J. Phys. A **16**(4) (1983), 811–827.
- [82] F. Peruggi, F. di Liberto, G. Monroy, *Phase diagrams of the q -state Potts model on Bethe lattices*. Phys. A **141**(1) (1987), 151–186.
- [83] I.J. Polmear, *Light alloys from traditional alloys to nanocrystals*, 2006, 4th edn, Burlington, MA: Elsevier Butterworth-Heinemann.
- [84] R.B. Potts, *Some generalized order-disorder transformations*. Proc. Cambridge Philos. Soc. **48** (1952), 106–109.
- [85] C. Preston, *Gibbs states on countable sets*, Cambridge University Press, London, (1974).

- [86] B. Radhakrishnan, G.B. Sarma, T. Zacharia, *Modeling the kinetics and microstructural evolution during static recrystallization-Monte Carlo simulation of recrystallization*. Acta Mater. **46** (1998), 4415–4433.
- [87] M.M. Rahmatullaev, *The existence of weakly periodic Gibbs measures for the Potts model on a Cayley tree*. Theor. Math. Phys. **180**(3) (2014), 1019–1029.
- [88] M.M. Rahmatullaev, *A weakly periodic Gibbs measure for the ferromagnetic Potts model on a Cayley tree*. Sib. Math. J. **56**(5) (2015), 929–935.
- [89] M.M. Rahmatullaev, *On weakly periodic Gibbs measures of the Potts model with a special external field on a Cayley tree*. Zh. Mat. Fiz. Anal. Geom. **12**(4) (2016), 302–314.
- [90] M.M. Rahmatullaev, *On weakly periodic Gibbs measures for the Potts model with an external field on a Cayley tree*. Ukrainian Math. J. **68**(4) (2016), 598–611.
- [91] M.A. Rasulova, *On periodic Gibbs measures for the Potts-SOS model on a Cayley tree*. Theoret. Math. Phys. **199**(1) (2019), 586–592.
- [92] J. Reichardt, S. Bornholdt, *Detecting fuzzy community structures in complex networks with a Potts model*. Phys. Rev. Lett. **93** (2004), Art. 218701, 4 pp.
- [93] N.F. Robertson, M. Pawelkiewicz, J.L. Jacobsen, H. Saleur, *Integrable boundary conditions in the antiferromagnetic Potts model*. J. High Energy Phys. **5** (2020), 144, 34 pp.
- [94] H.E. Rodriguez, P. Barrat-Charlaix, M. Weigt, *Toward inferring Potts models for phylogenetically correlated sequence data*. Entropy, **21**(11) (2019), Paper No. 1090, 20 pp.
- [95] B. Rosental, Z. Kozhekbaeva, N. Fernhoff, J.M. Tsai, N. Traylor-Knowles, *Coral cell separation and isolation by fluorescence-activated cell sorting*, BMC Cell Biology, **18**, 30 (2017).
- [96] U.A. Rozikov, *On pure phase of the anti-ferromagnetic Potts model on the Cayley tree*, Uzbek Math. J. No. 1 (1999), 73–77 (Russian).
- [97] U.A. Rozikov, *Description uncountable number of Gibbs measures for inhomogeneous Ising model*, Theor. Math. Phys. **188**(1) (1999), 77–84.
- [98] U. A. Rozikov, *On q -component models on Cayley tree: contour method*. Lett. Math. Phys. **71**(1) (2005), 27–38.
- [99] U.A. Rozikov, Y.M. Suhov, *Gibbs measures for SOS models on a Cayley tree*. Infin. Dimens. Anal. Quantum Probab. Relat. Top. **9** (2006), 471–488.
- [100] U.A. Rozikov, *A constructive description of ground states and Gibbs measures for Ising model with two-step interactions on Cayley tree*. J. Stat. Phys. **122**(2) (2006), 217–235.
- [101] U.A. Rozikov, *A contour method on Cayley trees*. J. Stat. Phys. **130**(4) (2008), 801–813.
- [102] U.A. Rozikov, F.T. Ishankulov, *Description of periodic p -harmonic functions on Cayley trees*, Nonlinear Diff. Equations Appl. **17**(2) (2010), 153–160.
- [103] U.A. Rozikov, *Gibbs measures on Cayley trees*. World Sci. Publ. Singapore. 2013.
- [104] U.A. Rozikov, R.M. Khakimov, *Periodic Gibbs measures for the Potts model on the Cayley tree*. Theor. Math. Phys. **175**(2) (2013), 699–709.
- [105] U.A. Rozikov, *Gibbs measures on Cayley trees: results and open problems*. Rev. Math. Phys. **25**(1) (2013), 1330001, 112 pp.
- [106] U.A. Rozikov, *Tree-hierarchy of DNA and distribution of Holliday junctions*, Jour. Math. Biology. **75**(6-7) (2017), 1715–1733.
- [107] U.A. Rozikov, M.M. Rahmatullaev, *On free energies of the Potts model on the Cayley tree*. Theor. Math. Phys. **190**(1) (2017), 98–108.
- [108] U.A. Rozikov, G.I. Botirov, *Non-translation invariant Gibbs measures for models with uncountable set of spin values on a Cayley tree*. Rep. Math. Phys. **81**(1) (2018), 105–115.
- [109] U.A. Rozikov, *Holliday junctions for the Potts model of DNA*. In book: Ibragimov Z. et.al (Eds). Algebra, Complex Analysis, and Pluripotential Theory. Springer Proceedings in Mathematics and Statistics. **264** (2018), 151–165.
- [110] U.A. Rozikov, R.M. Khakimov, F.Kh. Khaidarov, *Extremality of translation invariant Gibbs measures for Potts model on Cayley tree*. Theor. Math. Phys. **196**(1) (2018), 1043–1058.
- [111] U.A. Rozikov, *Thermodynamics of interacting system of DNAs*. Theor. Math. Phys. **206**(2) (2021), 174–183.
- [112] U.A. Rozikov, *Thermodynamics of DNA-RNA renaturation*. Int. J. Geom. Methods Mod. Phys. 2150096 (2021), 14 pages.
- [113] S. Sanyal, J.A. Glazier, *Viscous instabilities in flowing foams: A Cellular Potts Model approach*. J. Stat. Mech. Theory Exp. (2006), no. 10, P10008, 9 pp.

- [114] J. Salas, A.D. Sokal, *Absence of phase transitions for the antiferromagnetic Potts model via the Dobrushin uniqueness theorem*, J. Stat. Phys. **86** (1997), 551–579.
- [115] T.C. Schelling, *Dynamic models of segregation*. J. Math. Sociology **1** (1971), 143–186.
- [116] C. Schulze, *Potts-like model for ghetto formation in multi-cultural societies*. Int. J. Modern Phys. C. **16**(3) (2005), 351–355.
- [117] A. Shahraz, A. Borhan, K.A. Fichthorn, *Wetting on physically patterned solid surfaces: the relevance of molecular dynamics simulations to macroscopic systems*. Langmuir **29**(37) (2013), 11632–11639.
- [118] A. Shahraz, A. Borhan, K.A. Fichthorn, *Kinetics of droplet wetting mode transitions on grooved surfaces: forward flux sampling*. Langmuir **30**(51) (2014), 15442–15450.
- [119] A.N. Shiryaev, *Probability*, 2nd ed. Graduate Texts in Mathematics, **95**. Springer, New York, 1996.
- [120] Ya. G. Sinai, *Theory of phase transitions: Rigorous Results*, Pergamon, Oxford, (1982).
- [121] T.N. de Silva, V. Sivised, *A statistical mechanics perspective for protein folding from q-state Potts model*. arXiv:1709.04813.
- [122] A. Sly, *Reconstruction for the Potts model*. Ann. Probab. **39**(4) (2011), 1365–1406.
- [123] J. Srolvitz, M.P. Anderson, G.S. Grest, P.S. Sahni, *Grain growth in two-dimensions*, Scr. Metall., **17** (1983), 241–246.
- [124] M. Steel, M. Charleston, *Five surprising properties of parsimoniously colored trees*, Bull. Math. Biol. **57** (1995), 367–375.
- [125] L. Sun, Y.F. Chang, X. Cai, *A discrete simulation of tumor growth concerning nutrient concentration*. Int. J. Modern Phys. B **18** (2004), 2651–2657.
- [126] A. Szabó, R.M.H. Merks, *Cellular Potts modeling of tumor growth, tumor invasion, and tumor evolution*. Front. Oncol. **3** (2013), Art. 87, 12 pp.
- [127] T. Takaishi, *Simulations of financial markets in a Potts-like model*. Int. J. Modern Phys. C **16**(08) (2005), 1311–1317.
- [128] D.R. Tan, C.D. Li, W.P. Zhu, F.J. Jiang, *A comprehensive neural networks study of the phase transitions of Potts model*. New J. Phys. **22** (2020), 063016, (18 pages).
- [129] V. Tikare, J.D. Cawley, *Application of the Potts model to simulation of Ostwald ripening*. J. Amer. Ceramic Soc. **81**(3) (1998), 485–491.
- [130] P.N. Timonin, *Statistics of geometric clusters in Potts model: statistical mechanics approach*. Proc. A. **476**(2240) (2020), 215–228.
- [131] A. Voss-Böhme, *Cellular Potts models for interacting cell populations: Mathematical foundation, challenges, and future prospects*, Probabilistic cellular automata, 311–325, Emerg. Complex. Comput., 27, Springer, Cham, 2018.
- [132] M.J. de Vries, *Technological Processes*. In: Teaching about Technology. Contemporary Issues in Technology Education. Springer, (2016).
- [133] J. Wang, J. Wang, H.E. Stanley, *Multiscale multifractal DCCA and complexity behaviors of return intervals for Potts price model*. Phys. A **492** (2018), 889–902.
- [134] D. Weaire, F. Bolton, P. Molho, J. A. Glaziers, *Investigation of an elementary model for magnetic froth*. J. Phys.: Condens. Matter **3**(13) (1991), 2101–2115.
- [135] F.Y. Wu, *The Potts model*. Rev. Modern Phys. **54** (1982), 235–268.
- [136] D.Xiong, H.Zhao, *q-state Potts-glass neural network based on pseudoinverse rule*, J. Phys. A **43**(44) (2010), 445001, 9 pp.
- [137] K.Xu, J. Wang, *Weighted fractional permutation entropy and fractional sample entropy for nonlinear Potts financial dynamics*. Phys. Lett. A **381**(8) (2017), 767–779.

U. A. ROZIKOV

V.I.ROMANOVSKIY INSTITUTE OF MATHEMATICS OF UZBEK ACADEMY OF SCIENCES;
AKFA UNIVERSITY, 1ST DEADLOCK 10, KUKCHA DARVOZA, 100095, TASHKENT, UZBEK-
ISTAN;

FACULTY OF MATHEMATICS, NATIONAL UNIVERSITY OF UZBEKISTAN.

Email address: rozikovu@yandex.ru